1 **Cover page**

2

3 **Exploratory Data Analysis Recognizing Geometrical Patterns in Meta-analysis**

4

5 Keiichiro Kimoto, M.Sc.[1, 2 *], Munekazu Yamakuchi, M.D., Ph.D.[1], Kazunori Takenouchi, M.D., Ph.D. [1],

6 Teruto Hashiguchi, MD, Ph.D.[1]

7

8 [1] Department of Laboratory and Vascular Medicine, Kagoshima University Graduate School of Medical and

9 Dental Sciences, 8-35-1 Sakuragaoka, Kagoshima 890-8520, Japan

10 [2] Present Affiliation: External Advisor for Data Strategy Research Institute, Yokohama, Japan

11

12 *Corresponding author: Keiichiro Kimoto

13 Department of Laboratory and Vascular Medicine, Kagoshima University Graduate School of Medical and

14 Dental Sciences, 8-35-1 Sakuragaoka, Kagoshima 890-8520, Japan.

15 E-mail address: k1974142@kadai.jp

16 Phone: /Fax: +81-99-275-5437/+81-99-275-2629

17 Word count (text section): 2492 (summary text: 252, main text: 2240)

18

19

20 **Text**

21 **Summary text**

22 **Historically, Sir Isaac Newton, with a great perspective of geometry, analysed an elliptical**
23 **orbit derived from Kepler's primary astronomical data analysis, and the sir elicited the theory of**
24 **gravitation. Namely, secondary analysis with geometry was an essential step in physics. Then, with a**
25 **geometrical perspective, a re-analysis of a chart in the figure is also practical in biomedicine?**
26 **Nowadays, some image-checking AI detects research misconduct but not for useful, latent findings[1].**
27 **Taking our concept one step further, we focused on a geometrical meaning of the confidence interval**
28 **error bar. As an exploratory data analysis know-how in a figure of meta-regression analysis, we**
29 **conceived a method based on recognising geometrical patterns (layered hyperbolic shapes) suspected of**
30 **overlapping subgroups. Here we show the result that we applied our ideas to the traveller's thrombosis**
31 **(economy class syndrome) and coronavirus disease 2019 (COVID-19), both of which were suspected of**
32 **having overlooked information from many controversy[2-21]. Our analysis implied two S-curve types of**
33 **risk increasing during a flight in the traveller's thrombosis. Also, our analysis demonstrated overlooked**
34 **cyclic patterns on the onset of thrombosis. This result suggests a strong relationship between travel and**
35 **starting oral contraceptives (*e.g.*, honeymoon and starting birth control oral contraceptives), which**
36 **means that risk diversification might allow more safe use of oral contraceptives. In the COVID-19, our**
37 **analysis demonstrated unrecognised scatter plot patterns on cardiac biomarkers, which may serve**

studies for pathophysiology in COVID-19 patients. Regarding the above findings, pattern recognition of hyperbolic shapes can contribute to a significant discovery in data mining.

Main text

Recently, software improvements have allowed us to make a beautiful chart, but the understanding chart is required[22]. As readers of a scientific article, we took the idea of "reading a chart carefully" one step further and made a question that "something new exploratory data analysis (data mining) method assisted us to find important knowledge from previously published figures?". In addition, although statistics based on probability theory have applied the mathematical method to biomedicine (e.g., P-value), we turned our attention to the viewpoint of geometry regarding its importance in history.

Subsequently, we were interested in a research field, traveller's thrombosis, in which many controversies seemed to be associated with something overlooked **(Supplementary discussion 1: history of traveller's thrombosis)**. In the literature review, we focused on a figure that showed a result of meta-regression analysis (Chandra et al., *Ann Intern Med.* 2009;151(3):180-90., Figure 3)[7]. In this figure, we saw a geometrical shape (layered hyperbolic shapes) that seemed to be formed by overlapping two subgroups **(Fig. 1 a-d, Fig. 2, a)**.

Through those trains of thought, we conceived a methodological process based on our basic concept that approaching biomedical data from geometry was essential for exploratory data analysis. As know-how,

here we propose a kind of pattern recognition, which is searching for layered hyperbolic patterns in a figure showing a result of meta-regression analysis.

To validate our ideas, we worked on consecutive exploratory data analyses, such as Analysis 1 (1A, 1B) and Analysis 2, setting a working hypothesis that the shape formed by multiple subgroups for **(overall study framework is shown in Extended Data Fig. 1)**.

Numerical Experiment

Considering theoretical consideration and numerical experiment, we constructed three mathematical formulas for fitting hyperbolic patterns to data **(see Fig. 1 & Methods)**. The numerical experiment indicated that a U-shaped curve formed by the end of the confidence limit could be approximated by a parabola **(Fig. 1, c)**.

Analysis 1A (dataset: Chandra et al.)[7]

To assess eligibility for regression analysis, we reviewed a dataset, which was consisted of four study data gathered by Chandra et al.[7] for meta-regression analysis (Martinelli et al., 2003; Parkin et al., 2006; Cannegieter et al., 2006; Kuipers et al., 2007)[23-26]. In this assessment, two study data (Martinelli et al., 2003; Cannegieter et al., 2006)[23,25] were judged inappropriate and excluded. Also, the odds ratio reported by Parkin et al.[24] was suspected to be affected by a miscalculation, but qualitatively, it could only be used **(see Extended Data Fig. 1 & Methods)**.

In a part of the original dataset (Parkin et al., 2006 & Kuipers et al., 2007)[24,26], layered hyperbolic patterns appeared and applied regression analysis with the above three formulas. The inflexion points of the S-curves (centres of distributions) were 7.1 hours and 11.8 hours, respectively **(Fig. 2, b)**.

Notably, we observed an overlooked cyclic pattern in the figure reported by Cannegieter et al[25] during the data review process. The cycle was 27.4 days **(Extended Data Fig. 2)**. They did not mention this wave pattern, and this notable oversight allowed to be accounted for by an inappropriate 3-dimensional graph that disrupted human visual recognition **(Fig. 2, c, d, & Extended Data Fig. 2)**.

Analysis 1B (dataset: Philbrick et al.)[4]

Considering that only a few data were available for the first analysis, to validate the first result, we performed a similar analysis using another dataset, which was gathered by Philbrick et al. for a systematic review. As a preparation, we conducted a data review to confirm eligibility for regression analysis **(see Extended Data Fig. 1)**. Then, only S-curves were applied because the dataset did not contain risk ratio data, and hyperbolic shapes could not be fitted (for the details, see Methods). In this analysis, we found that two inflexion points of S-curves were divided similarly to the first analysis (< 10 hours, > 10 hours) in the stratified datasets by pulmonary embolism (PE) and deep vein thrombosis (DVT). The inflexion point of PE was about 9.2 hours, and the point of DVT was about 12.1 hours, respectively **(Extended Data Fig. 3)**.

Additionally, we found that unrecognised periodic pattern in the data reported by Clérel and Caillard[27] during the data review, which was suspected to be the effect of circadian rhythm **(Extended Data**

Fig. 4). We also found a post-travel cyclic pattern in the Kelman et al.[28] same cases as Cannegieter et al[25]. The wave was less clear than the wave observed in the data reported by Cannegieter et al[25]. In the waveform, there was a raw-risk period just before 90 days. In this data, there was an uptrend **(Extended Data Fig. 5)**.

Furthermore, we found a correlation between the stepped stages of increasing PE patients and the issuance of the guidelines[29-32] for preventive hormone replacement therapy (HRT) to a menopause woman in a figure reported by Clérel and Caillard[27] **(Extended Data Fig. 6)**.

Analysis 2 (dataset: COVID-19)[33]

Considering the above two analysis results, we decided to apply our ideas to the current complex COVID-19 pandemic problem to find some overlooked things because there was some controversy about the COVID-19 related thrombosis. This situation was similar to that of the traveller's thrombosis. **(Supplementary discussion 2: research situations of COVID-19 related thrombosis)**, and we started this analysis under the inspiration from the famous mathematician Polya who stated that solving a similar problem helped us solve a more difficult problem[34].

One of us (KK) searched for the layered hyperbolic pattern using a search engine and extracted a figure reported by Matsushita et al.[33] **(Fig. 3, a-c)**. After evaluating eligibility **(see Extended Data Fig. 1)**, patterns that allowed to be fitted hyperbolic shapes appeared **(Fig. 3, d-f, & g-i)**.

Considering the cause of these patterns, we found the matching between grouping the data by hyperbolic patterns and grouping by data cut-off days **(Extended Data Fig. 7)**. We calculated weighted

113 averages of age by grouping. In the earlier days group, non-severe was 46.5, severe was 57.7, and middle age
114 (45-64). In the late date group, non-severe was 40.9, and severe was 68.6, which were mature age (25-44) and
115 elderly (> 65), respectively.

116 Surprisingly, we found unrecognized patterns during the data review process in a figure reported by
117 Guo et al.[35], which showed a relationship between N-terminal pro-brain natriuretic peptide (NT-proBNP) and
118 Troponin T (TnT). There were three clusters of subgroup patterns, and each cluster could be fitted parabola
119 **(Fig. 4 a, b, Extended Data Fig. 8 & Extended Data Fig. 9)**.

120 The third subgroup pattern was similar to the pattern of ST-elevating myocardial infarction in the
121 figure report by Budnik et al[36]. That study was a comparative study between Takotsubo cardiomyopathy (also
122 known as stress cardiomyopathy or broken heart syndrome) and ST-elevating myocardial infarction. This tiled
123 parabola appeared in another study on COVID-19 patients[37], and the pattern had already appeared in other
124 studies[38,39] before the pandemic. However, those patterns were not recognised by each author.

125 Additionally, In the case of dropping points to the horizontal axis (troponin axis), the histogram on
126 the troponin axis results in bimodality. The above results matched the patterns reported by other studies
127 **(Extended Data Fig. 8)**[37,40,41].

128 Furthermore, by mounting the data of high-sensitivity C-Reactive protein (hsCRP) onto the third
129 subgroup and constructing a parabolic cylinder, we found a pattern that might further be subdivided into two
130 subgroups on the side surface of this parabolic cylinder **(Fig. 4, c, d, & Extended Data Fig. 10)**.

131

Discussion

Using pattern recognition of hyperbolic shape as a key to discoveries in exploratory data analysis, we started research for traveller's Thrombosis and COVID-19, and as a result, our concept of the geometrical viewpoint allowed us to discover many unrecognised patterns. Therefore, approaching data from geometry and exploring data focusing on hyperbolic patterns can be a practical option for researchers.

In traveller's thrombosis, we obtained consistent results from two analyses (7.1 hours and 11.8 hours vs 9.2 hours and 12.1 hours) **(Fig. 2, b, Extended Data Fig. 3)**. The discrepancy between the value of 7.1 hours and 8.5 hours seems to be explained by the miscalculation found in the data review process (see Methods). Although many researchers have led controversial discussions based on a single curve, our results implied two S-curves. We hypothesised two high-risk periods and two types of high-risk groups, which may have to be considered with the "factor V Leiden paradox"[42] **(Supplementary discussion 3: two high-risk periods and two types of high-risk groups?)**.

Another noteworthy point is the cyclic patterns (wave) **(Fig. 2, c, d)** and the raw-risk period just before 90 days in Kelman et al.[27] **(Extended Data Fig. 5).** In Cannegieter et al.[24], the cyclic pattern disappeared around 90 days, consistent with that the high-risk period in oral contraceptive (OC) use was the first three months (90 days)[42]. Also, the above raw-risk period explains extended-use type OC, which has a planned drug withdrawal, such as 84 active days and seven placebo days[43-45]. In addition, the uptrend in the data by Kelman et al.[27] could be explained by depot agent type OC administrated 90 days cycle[46]. So, our findings imply that the 28 days cycle OC is attributable to the cyclic pattern, and both cycle type and

151 extended-use type OC use is triggered by travel. An opposition may arise considering that both of relative risk
152 reported by Martinelli et al.[22] and Cannegieter et al.[24] were low **(Fig. 2, b)**, but it seems to be explained by
153 bias derived from using their partner as control **(Supplementary discussion 4: OC users and bias by their**
154 **partner)**.

155 A halfway cycle (17.9 days) in Kelman et al.[28] was explained by a mixture of the 28 days OC cycle
156 and a type of HRT cycle (sequential type; daily estrogen dosing and 10–14 days progestogen)[46]. Also, another
157 problem is that the wave in Cannegieter et al. was clear (thrombosis onset: March 1999-March 2000)[25].
158 However, the wave in Kelman et al. (1981-1999)[28] was not clear despite the exposures in Cannegieter et al.
159 (air travel, train, bus, and 48.5% car trip)[25] was more complex than Kelman et al. (only air travel)[28], was
160 answered by the history of HRT. In Kelman et al.[28], there might be both young women taking OC and
161 menopausal women receiving HRT, but only OC users might remain after the HERS study reported risk of
162 HRT (1998)[31], which was assisted by the growth of thrombosis onset slowed at the HERS study[31] **(Extended**
163 **Data Fig. 6)**. Also, the above cars might be honeymoon cars. Although it was not decreasing, the result might
164 be caused by some woman's desire for joyful travel to Paris with HRT.

165 Our thought on pharmacoepidemiology in the real world, starting OC or HRT was triggered by
166 travel and decision making of HRT connected to travel, which means that well-planned usage based on risk
167 diversification may allow more safe use of OC and HRT.

168 In appreciation of our ideas to COVID-19, the dataset grouping by Matsushita et al.[32] matched the
169 grouping by data cut-off dates **(Extended Data Fig. 7)**, and age structure diverged from middle age to mature

and elderly, which was consistent with the hypothesis that COVID-19 spread from the seafood market. Middle-aged people might go into the workforce for manual labour treating fish containers, mature people might want to select IT jobs, and elderly people might stay in the house.

Interestingly, our analysis of the data by Guo et al.[34] showed three clusters of subgroups, and one of those formed the tilted parabola. Also, the patterns matched the other studies **(Fig. 4 a, b, Extended Data Fig. 8 & Extended Data Fig. 9)**[36-41]. Considering the study by Budnik et al.[36], those subgroups may have different biological mechanisms.

Additionally, we found patterns on the side surface of this parabolic cylinder **(Fig. 4, c, d, & Extended Data Fig. 10)**. A paradoxical result on troponin was obtained just before the pandemic[48], and Meisel et al. mentioned that the CRP to troponin ratio (CRP/troponin) could serve to differentiate between myopericarditis and acute myocardial ischemia (AMI), although not the study on COVID-19 patients. In COVID-19, Caro-Codón et al. reported interesting behaviour of CRP[35]. Also, a meta-analysis by Lagunas-Rangel reported that the lymphocyte-to-C-reactive protein ratio (LCR) level, which was not a simple measurement value but a ratio, might be related to an inflammatory process[47].

The above studies might imply complex data structures in 2-dimensional and 3-dimensional scatter plots consisting of biomarker values, and our findings may serve cardiac biomarkers' research field.

Supplementary, we explain the misuse of linear regression analysis in the study by Guo et al.[35] **(Supplementary discussion 5: misuse of linear regression analysis).**

188 Although many studies on visualization of meta-analysis have been conducted[48], our simple idea
189 (hyperbolic pattern) has not been proposed. As named “error”, researchers usually view an error bar
190 negatively. Also, in the wheel's history, an invention of carriages, which was achieved by arranging the
191 wheels in parallel, appeared in ancient times, but the idea of the bicycle, which was innovatively arranging
192 wheels vertically, had not been conceived before the 19th century[49,50]. Those mental blocks might have made
193 it hard to imagine that vertical error bars provided information on a horizontal axis.
194 Evaluating our ideas, we discovered many oversights which were entirely beyond the initial scope.
195 Appearing overlapped hyperbolic patterns may show poor data review and analysis. Currently, pattern
196 recognition based on Artificial Intelligence (AI) detects cancer sites from images. Considering our discoveries
197 by an analogy that Newton's theory enabled the prediction of a planet's orbit, implementing our idea (a kind of
198 mathematical model or theory) in an AI system might assist another discovery of clinical issues.
199

Main references

1 Van Noorden, R. Journals adopt AI to spot duplicated images in manuscripts. *Nature*, doi:10.1038/d41586-021-03807-6 (2021).

2 Adi, Y., Bayliss, S., Rouse, A. & Taylor, R. S. The association between air travel and deep vein thrombosis: systematic review & meta-analysis. *BMC Cardiovasc Disord* **4**, 7, doi:10.1186/1471-2261-4-7 (2004).

3 Kuipers, S. *et al.* Travel and venous thrombosis: a systematic review. *J Intern Med* **262**, 615-634, doi:10.1111/j.1365-2796.2007.01867.x (2007).

4 Philbrick, J. T., Shumate, R., Siadaty, M. S. & Becker, D. M. Air travel and venous thromboembolism: a systematic review. *J Gen Intern Med* **22**, 107-114, doi:10.1007/s11606-006-0016-0 (2007).

5 Spencer, F. A. Review: Flight times >8 hours and presence of risk factors for VTE increases travel related VTE. *Evid Based Med* **12**, 105, doi:10.1136/ebm.12.4.105 (2007).

6 Trujillo-Santos, A. J., Jiménez-Puente, A. & Perea-Milla, E. Association between long travel and venous thromboembolic disease: a systematic review and meta-analysis of case-control studies. *Ann Hematol* **87**, 79-86, doi:10.1007/s00277-007-0373-8 (2008).

7 Chandra, D., Parisini, E. & Mozaffarian, D. Meta-analysis: travel and risk for venous thromboembolism. *Ann Intern Med* **151**, 180-190, doi:10.7326/0003-4819-151-3-200908040-00129 (2009).

8 Vandenbroucke, J. P., Cannegieter, S. C. & Rosendaal, F. R. Travel and venous thrombosis: an exercise in thinking about bias. *Ann Intern Med* **151**, 212-213, doi:10.7326/0003-4819-151-3-200908040-00130 (2009).

9 Gore, J. M. in *NEJM Journal Watch* (2009).

10 Ebimayo-no-kai (Evidence-Based Journal club for residents) in Tokyo-Kita Medical Center. *Web Page from the Ebimayo-no-kai (Evidence-Based Journal club for residents) in Tokyo-Kita Medical Center*, 2009).

11 American College of Chest Physicians. (2012).

12 Crowther, M. (ed American College of Chest Physicians) (2012).

13 Kahn, S. R. *et al.* Prevention of VTE in nonsurgical patients: Antithrombotic Therapy and Prevention of Thrombosis, 9th ed: American College of Chest Physicians Evidence-Based Clinical Practice Guidelines. *Chest* **141**, e195S-e226S, doi:10.1378/chest.11-2296 (2012).

14 Schünemann, H. J. *et al.* American Society of Hematology 2018 guidelines for management of venous thromboembolism: prophylaxis for hospitalized and nonhospitalized medical patients. *Blood Adv* **2**, 3198-3225, doi:10.1182/bloodadvances.2018022954 (2018).

15 Clark, S. L., Onida, S. & Davies, A. Long-haul travel and venous thrombosis: What is the evidence? *Phlebology* **33**, 295-297, doi:10.1177/0268355517717423 (2018).

16 Ahmed, S., Zimba, O. & Gasparyan, A. Y. Thrombosis in Coronavirus disease 2019 (COVID-19) through the prism of Virchow's triad. *Clin Rheumatol* **39**, 2529-2543, doi:10.1007/s10067-020-05275-1 (2020).

17 Barrett, C. D., Moore, H. B., Yaffe, M. B. & Moore, E. E. ISTH interim guidance on recognition and management of coagulopathy in COVID-19: A comment. *J Thromb Haemost* **18**, 2060-2063, doi:10.1111/jth.14860 (2020).

18 Callaway, E., Ledford, H. & Mallapaty, S. Six months of coronavirus: the mysteries scientists are still racing to solve. *Nature* **583**, 178-179, doi:10.1038/d41586-020-01989-z (2020).

19 Tal, S., Spectre, G., Kornowski, R. & Perl, L. Venous Thromboembolism Complicated with COVID-19: What Do We Know So Far? *Acta Haematol* **143**, 417-424, doi:10.1159/000508233 (2020).

20 Marietta, M., Coluccio, V. & Luppi, M. COVID-19, coagulopathy and venous thromboembolism: more questions than answers. *Intern Emerg Med* **15**, 1375-1387, doi:10.1007/s11739-020-02432-x (2020).

21 Rothman, K. J. Thrombosis after travel. *PLoS Med* **3**, e300, doi:10.1371/journal.pmed.0030300 (2006).

22 Cairo, A. (W. W. Norton & Company, New York, 2019).

23 Martinelli, I. *et al.* Risk of venous thromboembolism after air travel: interaction with thrombophilia and oral contraceptives. *Arch Intern Med* **163**, 2771-2774, doi:10.1001/archinte.163.22.2771 (2003).

24 Parkin, L., Bell, M. L., Herbison, G. P., Paul, C. & Skegg, D. C. Air travel and fatal pulmonary embolism. *Thromb Haemost* **95**, 807-814 (2006).

25 Cannegieter, S. C., Doggen, C. J., van Houwelingen, H. C. & Rosendaal, F. R. Travel-related venous thrombosis: results from a large population-based case control study (MEGA study). *PLoS Med* **3**, e307, doi:10.1371/journal.pmed.0030307 (2006).

26 Kuipers, S. *et al.* The absolute risk of venous thrombosis after air travel: a cohort study of 8,755 employees of international organisations. *PLoS Med* **4**, e290, doi:10.1371/journal.pmed.0040290 (2007).

27 Clérel, M. & Caillard, G. [Thromboembolic syndrome from prolonged sitting and flights of long duration: experience of the Emergency Medical Service of the Paris Airports]. *Bull Acad Natl Med* **183**, 985-997; discussion 997-1001 (1999).

28 Kelman, C. W. *et al.* Deep vein thrombosis and air travel: record linkage study. *BMJ* **327**, 1072, doi:10.1136/bmj.327.7423.1072 (2003).

29 Guidelines for counseling postmenopausal women about preventive hormone therapy. American College of Physicians. *Ann Intern Med* **117**, 1038-1041, doi:10.7326/0003-4819-117-12-1038 (1992).

30 Smith, S. C. *et al.* AHA consensus panel statement. Preventing heart attack and death in patients with coronary disease. The Secondary Prevention Panel. *J Am Coll Cardiol* **26**, 292-294, doi:10.1016/0735-1097(95)90846-g (1995).

31 Hulley, S. *et al.* Randomized trial of estrogen plus progestin for secondary prevention of coronary heart disease in postmenopausal women. Heart and Estrogen/progestin Replacement Study (HERS) Research Group. *JAMA* **280**, 605-613, doi:10.1001/jama.280.7.605 (1998).

32 Rossouw, J. E. *et al.* Risks and benefits of estrogen plus progestin in healthy postmenopausal women: principal results From the Women's Health Initiative randomized controlled trial. *JAMA* **288**, 321-333, doi:10.1001/jama.288.3.321 (2002).

33 Matsushita, K. *et al.* The Relationship of COVID-19 Severity with Cardiovascular Disease and Its Traditional Risk Factors: A Systematic Review and Meta-Analysis. *Glob Heart* **15**, 64, doi:10.5334/gh.814 (2020).

34 Polya, G. *How to Solve It: A New Aspect of Mathematical Method (Princeton Science Library)*. (Princeton University Press, 1957).

35 Guo, T. *et al.* Cardiovascular Implications of Fatal Outcomes of Patients With Coronavirus Disease 2019 (COVID-19). *JAMA Cardiol* **5**, 811-818, doi:10.1001/jamacardio.2020.1017 (2020).

36 Budnik, M. *et al.* Simple markers can distinguish Takotsubo cardiomyopathy from ST segment elevation myocardial infarction. *Int J Cardiol* **219**, 417-420, doi:10.1016/j.ijcard.2016.06.015 (2016).

37 Wang, Y. *et al.* Cardiac Injury and Clinical Course of Patients With Coronavirus Disease 2019. *Front Cardiovasc Med* **7**, 147, doi:10.3389/fcvm.2020.00147 (2020).

38 Sugawa, S., Masuda, I., Kato, K. & Yoshimura, M. Increased Levels of Cardiac Troponin I in Subjects with Extremely Low B-type Natriuretic Peptide Levels. *Sci Rep* **8**, 5120, doi:10.1038/s41598-018-23441-z (2018).

39 Satyan, S., Light, R. P. & Agarwal, R. Relationships of N-terminal pro-B-natriuretic peptide and cardiac troponin T to left ventricular mass and function and mortality in asymptomatic hemodialysis patients. *Am J Kidney Dis* **50**, 1009-1019, doi:10.1053/j.ajkd.2007.08.017 (2007).

40 Caro-Codón, J. *et al.* Characterization of NT-proBNP in a large cohort of COVID-19 patients. *Eur J Heart Fail* **23**, 456-464, doi:10.1002/ejhf.2095 (2021).

41 Demir, O. M. *et al.* Impact and Determinants of High-Sensitivity Cardiac Troponin-T Concentration in Patients With COVID-19 Admitted to Critical Care. *Am J Cardiol* **147**, 129-136, doi:10.1016/j.amjcard.2021.01.037 (2021).

42 van Langevelde, K., Flinterman, L. E., van Hylckama Vlieg, A., Rosendaal, F. R. & Cannegieter, S. C. Broadening the factor V Leiden paradox: pulmonary embolism and deep-vein thrombosis as 2 sides of the spectrum. *Blood* **120**, 933-946, doi:10.1182/blood-2012-02-407551 (2012).

43 Wiegratz, I. *et al.* Effect of extended-cycle regimen with an oral contraceptive containing 30 mcg ethinylestradiol and 2 mg dienogest on bleeding patterns, safety, acceptance and contraceptive efficacy. *Contraception* **84**, 133-143, doi:10.1016/j.contraception.2011.01.002 (2011).

44 Loudon, N. B., Foxwell, M., Potts, D. M., Guild, A. L. & Short, R. V. Acceptability of an oral contraceptive that reduces the frequency of menstruation: the tri-cycle pill regimen. *Br Med J* **2**, 487-490, doi:10.1136/bmj.2.6085.487 (1977).

45 Legro, R. S. A Review of Extended-Cycle Oral Contraception. (Morrisville, North Carolina, USA, 2003).

46 Humans, I. W. G. o. t. E. o. C. R. t. Combined estrogen-progestogen contraceptives and combined estrogen-progestogen menopausal therapy. *IARC Monogr Eval Carcinog Risks Hum* **91**, 1-528 (2007).

47 Lagunas-Rangel, F. A. Neutrophil-to-lymphocyte ratio and lymphocyte-to-C-reactive protein ratio in patients with severe coronavirus disease 2019 (COVID-19): A meta-analysis. *J Med Virol* **92**, 1733-1734, doi:10.1002/jmv.25819 (2020).

48 Kossmeier, M., Tran, U. S. & Voracek, M. Charting the landscape of graphical displays for meta-analysis and systematic reviews: a comprehensive review, taxonomy, and feature analysis. *BMC Med Res Methodol* **20**, 26, doi:10.1186/s12874-020-0911-9 (2020).

49 Brunner, B. in *The Smart Set (online magazine)* (Drexel University, Philadelphia, 2017).

50 Japanese Wikipedia contributors (Wikipedia (Japanese site), 2021).

Methods

1. Numerical experiment

Unavoidably, this study conducted a numerical experiment to determine what curve approximates an edge of a confidence limit **(Fig. 1, c)**.

Generally, a dose-response relationship often indicates an S-curve. Considering the distribution of a population at thrombosis risk and the cumulative thrombosis onset, each of those is monomodal distribution and the S-shaped curve, respectively. So, we decided to use the sigmoid function, which is generally used in curve fitting to dose-response data, as the formula for the S-curve fitting.

Contrastively, the curve expressing the end of a confidence interval (confidence limit) is a sum of the S-shaped curve and U-shaped curve because the width of the confidence interval narrows near the centre of distribution due to many cases around the points. Similarly, the confidence interval widens at the distribution edge due to the small number of cases **(see Fig. 1, d)**.

Based on the above consideration, we selected the parabola as a candidate for the U-shaped curve because this curve was mathematically easy to handle (just junior high school level mathematics). So, we examined the validity of using parabola. However, mathematical proof of our conjecture was difficult because normal distribution was continuous probability distribution. So, we used a kind of discrete probability distribution, binomial distribution, to prove our conjecture experimentally because normal distribution could be approximated by binominal distribution. This idea was thinking in reverse of the usual statistical technique.

346 To generate binomial distribution data, we used the "BINOM.DIST" function, which is a function
347 for calculating the probability of binomial distribution in a kind of spreadsheet software, Microsoft Excel®
348 (Microsoft Corporation, Redmond, Washington, US).
349
350 **2. Equations for regression analysis**
351 The equations for the S-shaped curve, the upper end of the confidence limit, and the lower end of the
352 confidence limit, those equations are the following (1), (2), and (3), respectively. Note that in the below
353 equations, the coefficient L is generally set as 1. So we used this equation under the condition as L=1 unless
354 there is some reason.
355

356 $$y = \left\{\frac{K_1}{1+e^{L(x-M)}} + K_2\right\} \quad (1)$$

357 $$y = \left\{\frac{K_1}{1+e^{L(x-M)}} + K_2\right\} + (ax^2 + bx + c) \quad (2)$$

358 $$y = \left\{\frac{K_1}{1+e^{L(x-M)}} + K_2\right\} - (ax^2 + bx + c) \quad (3)$$

359
360 Also, a complete square of the quadratic function that represents the parabola is the following equation (4).
361

362 $$ax^2 + bx + c = a\left(x + \frac{b}{2a}\right)^2 - \frac{b^2-4ac}{4a} \quad (4)$$

363
364 Besides, the point P is the apex of the parabola is the following (5).

$$\mathrm{P}\left(-\frac{b}{2a}, -\frac{b^2-4ac}{4a}\right) \quad (5)$$

The following equations are the formula that expresses the outline of the distribution obtained by differential calculation on the S-shaped curve (6).

$$\frac{dy}{dx} = -\frac{K_1 L e^{L(x-M)}}{\left\{e^{L(x-M)}+1\right\}^2} \quad (6)$$

3. Analysis tools in this study

Reading values from the published figures were performed using the public domain software ImageJ in the public domain (https://imagej.net/Welcome). Regression analysis was performed using Python (Python Software Foundation, Delaware, USA https://www.python.org/psf/records/incorporation/). At this time, Python's functional modules NumPy (NumFOCUS sponsored open-source project, https://numpy.org/), Pandas (NumFOCUS sponsored open-source project, https://pandas.pydata.org/), SciPy (NumFOCUS sponsored open-source project, https://www.scipy.org/) and Matplotlib (NumFOCUS sponsored open-source project, https://matplotlib.org/) were also used. Additionally, a function as "Chart option" of Microsoft Excel® , which was shown in the "Trendline Options" section contained in "Format Trendline," was used. In the case of symbolic formula manipulation was required, formula manipulation software wxMaxima (Project Maxima maintained by 27 volunteers, https://maxima.sourceforge.io/) was used.

4. Analysis 1A (dataset: Chandra et al.)[7]

1) Data review to validate eligibility for regression analysis

a. The process of data review in this analysis

As the first step, we performed data mapping. In the figure of meta-regression analysis reported by Chandra et al.[7], it was not described what the data points correspond to the four original papers (Martinelli et al., 2003; Parkin et al., 2006; Cannegieter et al., 2006 and Kuipers et al., 2007)[23-26]. So, we measured the positions of each point and compared them with the original descriptions in the papers. In the second step, we performed a data review, which was an examination of the accuracy of cited values, and appropriately from the viewpoint of biomedicine. Our re-calculation confirmed the odds ratio (OR), confidence interval of the OR, and adjusted OR. In examining the values, we did not confirm Chandra et al.[7] and the four authors[23-26] because Chandra et al. described that each author did not respond to inquiry[7]. As a final step, we performed regression analysis using the eligible data for using regression analysis.

b. Data review

The data review showed some problems in the research reported by Cannegieter et al. and Martinelli et al.[23,25], and we excluded those data in the regression analysis. Also, there was a point to notice in the data reported by Parkin et al.[24] **(see Extended Data Fig. 1)**.

In confirming the accuracy of the values, there were no problems with the two studies (Kuipers et al. and Cannegieter et al.)[25,26], but there were problems in the other two studies **(Martinelli et al. and Parkin et al.)[23,24]**.

In Martinelli et al.[23], the problem was gender imbalance and unadjusted OR. In addition, although there were no explanations for the odds ratio described in the text cited by Chandra et al[7], the above OR was presumed to be an unadjusted value, judging from the context. Comprehensively, judging from both calculation results and the original article, the odds ratio cited by Chandra et al.[7] was strongly suspected of being an unadjusted value.

In Parkin et al.[24], there was a discrepancy between the OR and the described OR calculated by us. Also, it was suspected that cells in the cross table were mistaken (*e.g.*, in the table of Fig. 1a, the cell for control and the cell for total were mistaken). However, the error bar's length was relatively small since the total number of cases was notably smaller than other studies. So, qualitatively, it could only be used to group data to find hyperbolic patterns.

In confirming from the viewpoint of the biomedicine side, there were no problems with two studies (Kuipers et al. and Parkin et al.)[24,26], but there were problems in the other two studies **(Martinelli et al. and Cannegieter et al.)[23,25]**. In Martinelli et al.[23], judging from the subtitle, "interaction with thrombophilia and oral contraceptives," oral contraceptive (OC) bias was suspected. Initially, the study aimed to evaluate the interaction between OC use and travel. Considering the above, the OR had to be considered a value that contained a strong bias **(see also Supplementary discussion 4: OC users and bias by their partner)**. In

Cannegieter et al.[25], the data contained car travel, and the other studies contained only air travel. So exposure factors were different, and there was a problem from the viewpoint of comparability (e.g., air pressure, dehydration, and time difference). Also, Chandra et al.[7] showed two types of analysis results, including Cannegieter et al.[25] and not. Besides, the cyclic pattern could be explained by OC use was observed **(see Fig. 2, c & d)**. Also, Cannegieter et al.[25] did not adjust the OR by sex and OC use. So, it was strongly suspected that there was a strong bias derived from the different types of exposure factors and OC.

Judging from the above two types of data reviews, we excluded the data reported by two studies **(Martinelli et al. and Parkin et al.)**[23,24]. In the data reported by Kuipers et al.[26], there was no problem. The data reported by Parkin et al.[24] seemed to be used only for the purpose described above.

Interestingly, in four studies used in meta-regression analysis by Chandra et al.[7], all the first authors' names seem to be women's names ("Suzanne" Cannegieter[25], "Saskia" Kuipers[26], "Ida" Martinelli[23], "Lianne" Parkin[24]).

2) Regression Analysis

For the data judged as eligible, hyperbolic patterns were visually searched, and each data point was grouped into two groups. Then, a non-linear regression analysis using the formulas above was performed. In the fitting of the U-shaped curve, since there were many unknown coefficients for the number of data (there are seven unknowns, K_1, K_2, M, a, b, and c. in the equations (2) and (3)), the S-curve was fitted first, and the

remaining unknown coefficients (a, b, c) were fitted to the residuals of the S-curve fitting (see equation (2) and (3)).

3) Additional analysis

As described above, the cyclic pattern in the data reported by Cannegieter et al.[25] was observed, and we performed additional analysis. To conduct an appropriate non-linear regression analysis, we made an equation by combining two types of equations. The exponential decay equation was usually used to express radioactive decay in physics and clearance in medicine. The other was a trigonometric function (sine function) to express waveforms. The equation is shown in as below equation (7). Also, this scientific model (model formula) was used to estimate the ratio of patients by integral calculation.

$$y = N_1 e^{-\lambda_1 (t-b)} + N_2 e^{-\lambda_2 (t-b)} \mathrm{Asin}\{B(t-b)\} \quad (7)$$

The data reported as a bar graph was weekly data **(see Fig. 2, c and Extended Data Fig. 2)**. So, the week was converted into the number of days before the analysis, such as; the day getting off the vehicle was set as days 0, the first week was set as days 4, the second week was set as days 4 + 7, and the third week was set as days 4 + 7 × two, and the Nth week was set as days 4 + 7 × N.

Supplementary, according to the original description by Cannegieter et al.[25], 68 patients developed thrombosis in the first week, and "233" patients developed thrombosis within eight weeks after travelling.

458 However, there was a slight discrepancy in the values read from the bar graph. The value in our measurement
459 within eight weeks after travelling was "234", but the effect of only one patient was allowed to be regarded as
460 small (the description of 68 patients was the same.).

461 Cannegieter et al. described the number of patients who travelled with their partners to evaluate the
462 effect of OC (Cannegieter et al., PLoS Med. 2006 Aug;3(8):e307., Table 2)[25]. We found some mismatches for
463 the number of patients in the table, and the overall discrepancy was only one person by offset, and
464 Cannegieter et al. described that there were derived from missing value[25]. The mismatch between our
465 measurement and description might be related to the described explanation.

466

467 **5. Analysis 1B (dataset: Philbrick et al.)[4]**

468 1) Dataset search and data review

469 a. Dataset search

470 To validate the result of analysis 1A, we searched another dataset from meta-analysis or systematic
471 review on the traveller's thrombosis. To conduct this search, we used PubMed® setting the following search
472 keywords: "economy class syndrome [Title] " OR "traveler's [Title] AND thrombosis [Title]" OR "traveler's
473 [Title] AND thromboembolism [Title]" OR "flight [Title] AND thrombosis [Title]" OR "flight [Title] AND
474 thromboembolism [Title]" OR "flight-related [Title] AND thrombosis [Title]" OR "flight-related [Title] AND
475 thromboembolism [Title]" OR "travel [Title] AND thrombosis [Title]" OR "travel [Title] AND

476 thromboembolism [Title]" OR "travel-related [Title] AND thrombosis [Title]" OR "travel-related [Title] AND
477 thromboembolism [Title]" (Filters: Meta-Analysis, Systematic Review).

478 As a result, we obtained the eight articles (da Silva LF et al. *J Vasc Bras.* 2021 10;20:e20200164;
479 Benhaberou-Brun *Perspect Infirm.* 2010 7(3):16-7; Chandra et al. *Ann Intern Med.* 2009 151(3):180-90;
480 Kuipers et al. *J Intern Med.* 2007 262(6):615-34; Philbrick et al. *J Gen Intern Med.* 2007 22(1):107-14; Hsieh
481 et al. *J Adv Nurs.* 2005 51(1):83-98; Ansari et al. *J Travel Med.* 2005;12(3):142-54; Adi et al. *BMC*
482 *Cardiovasc Disord.* 2004 19;4:7).

483 Subsequently, we selected articles containing available abstracts on PubMed® online, confirming the
484 contents. As a candidate for our analysis, we selected a systematic review reported by Philbrick et al.[4]. The
485 study was taken up by the ACP Journal Club of the American College of Physicians[5] and another journal
486 club[10]. So, it seemed to be a highly reputed study. Therefore, we regarded that the dataset contained in the
487 research was suitable for validation.

488 Also, the research contained two lists of tables, one of which was a cohort studies dataset, and the
489 other was the case-control studies. However, the case-control studies had many different exposure factors. So,
490 we decided to use only the cohort studies dataset.

491

492 b. Data review

493 In the data review process, we reviewed the table containing ten cohort studies[27,28,51-58] and found
494 seven eligible cohort studies[27,51,54-58] for regression analysis. In Gajic et al. and Kelman et al., the only

495 distances were described[28,52], and Hughes et al. reported duration data for not per one flight (e.g., mean 39.4
496 h)[53], so time data for regression analysis was unavailable.

497 Additionally, although Philbrick et al. described that incidence per million was 0.5 in table 2 of their
498 article[4], the number was incorrect because it was based on only 1998. In the original description, Clérel &
499 Caillard mentioned that "According to the number of the passengers landing in the Aeroports de Paris, the
500 incidence during 1998 is 0.5 per million passengers"[27].

501

502 2) Regression Analysis

503 For the seven studies, data stratified by Pulmonary Embolism (PE) and Deep Vein Thrombosis
504 (DVT), regression analysis was performed using an S-shaped curve formula (see equation (1)). In the case of
505 curve-fitting on DVT data, we cancelled the setting of coefficient L=1 to increase the degree of freedom of the
506 S-curve **(Extended Data Fig. 3, b)**. To show the error bar in the figure **(Extended Data Fig. 3)**, we did not
507 use the values of confidence limits described in the report by Philbrick et al.[4], but values were re-calculated
508 from the number of cases using Wilson's method because data review result described above showed the error
509 of values at the citation.

510 In the seven studies, not OR or relative risk (RR), only the data indicating the incidence rate of
511 thrombosis was available. So, the hyperbolic pattern did not appear in the figure theoretically, and we
512 performed only the S-shaped curve fitting. This mechanism is explanted from the following calculation on a
513 confidence interval of a ratio.

514 The formula for a 95% confidence limit of a ratio using binomial approximation is expressed by the

515 following formula: P is a ratio, and N is the number of trials.

516

517 $$P - 1.96\frac{\sqrt{P(1-P)}}{\sqrt{N}} \leq P \leq P + 1.96\frac{\sqrt{P(1-P)}}{\sqrt{N}} \quad (8)$$

518

519 In the above equation, the fraction's numerator is not a constant value and does not depend on only the N,

520 which is associated with a data point's position in a population **(see Fig. 1)**.

521 In this regression analysis, converting time categories to time points was necessary, so we performed

522 this in three directions. The first one was taking the midpoint if the category was not the end of a category

523 sequence (e.g., 10-15 h could be converted to 12.5 h). The second one was taking the midpoint between the

524 time point of 0 and the lower limit of the category if the category was the lower end of a category sequence

525 (e.g., <3 h could be converted to 1.5 h). The third one was taking the sum of the value of the upper limit and

526 the value of the midpoint between the time point of 0 and the lower limit of the category sequence if the

527 category was the upper side of a category sequence (e.g., > 12 h could be converted to 12 h + 1.5 h =13.5 h).

528 Details of conversions are shown below (the original time category is shown in brackets).

529 Belcaro et al. [10-15 h]: 12.5 h (Belcaro, G. et al., *Angiology.* 2001;52(6):369-74.)[51]; Clérel et al.

530 [12.7 h]: 12.7 h (Clérel, M., & Caillard, G., *Bull Acad Natl Med.* 1999;183(5):985-97.)[27]; Jacobson et al. [11

531 h]: 11 h; Lapostolle et al. [<3 h, 3-6 h, 6-9 h, 9-12 h,> 12 h]: 1.5 h, 4.5 h, 7.5 h, 10.5 h, 13.5 h (12 + 1.5 = 13.5

532 h) (Jacobson, B.F. et al., *S Afr Med J.* 2003;93(7):522-8.)[54]; Pérez-Rodríguez et al. [<6 h, 6-8 h,> 8 h]: 3 h, 7

h, 11 h (8 + 3 = 11 h) (Pérez-Rodríguez, E. et al., *Arch Intern Med.* 2003;163(22):2766-70.)[56]; Schwarz et al. 2002 [> 8 h]: 12 h (midpoint of 0-8 h is 4 h and 8 + 4 = 12 hours) (Schwarz, T. et al., *Blood Coagul Fibrinolysis.* 2002;13(8):755-7.)[57]; Schwarz et al. 2003 [> 8 h]: 12 h (midpoint of 0-8 h is 4 h and 8 + 4 = 12 hours) (Schwarz, T. et al., *Arch Intern Med.* 2003 2003;163(22):2759-64.)[58].

3) Additional analysis

a. Regression analysis (data: Kelman et al.[28])

In the review process, a cyclic pattern was observed. So, we worked on regression analysis. Considering that onset of thrombosis tends to increase again, an equation upward-sloping curve was added to equation (7). The equation is the following (9).

$$y = N_1 e^{-\lambda_1 (t-b)} + N_2 e^{-\lambda_2 (t-b)} \mathrm{Asin}\{B(t-b)\} + (ax^2 + bx + c) \quad (9)$$

b. Analysis by using correlogram (data: Clérel & Caillard[27])

We considered using the "correlogram" in this study because it was more practical than observing the original data's fluctuation. Periodic fluctuation patterns may be unclear when looking at the original data alone, but potential patterns can be obtained using a correlogram, a data visualization method for analyzing time-series data. Also, as the correlation coefficient plotted on the correlogram, we decided to use Spearman's rank correlation coefficient instead of Pearson's product-moment correlation coefficient, which is easily

552 affected by outliers. Also, we performed a non-linear regression analysis using a mathematical formula (10)
553 that includes two sine functions.
554
555 $$y = n_1 \sin\{a_1(x - b_1)\} + n_2 \sin\{a_2(x - b_2)\} \quad (10)$$
556
557 In correlogram creation, firstly, a combination of data (data X1, data X1) was created by arranging
558 the original time series data (data X1) and a new combination (data X1, data X1') was created by shifting one
559 of them. Secondary, the correlation coefficient (also called the auto-correlation coefficient) between the
560 original time-series data (data X1) and the sifted time-series data (data X1'), except at the ends of two types of
561 time-series data where some correspondence could not be formed. By repeating shifting the time string data
562 and calculating the correlation coefficient, the locus of the correlation coefficient becomes the shape of waves.
563 Firstly (original waves of time strings are overlapped), the correlation coefficient is 1, and the value of the
564 correlation coefficient gradually decreases as the distance of the overlap increases. Finally (the wave is
565 inverted), the correlation coefficient is -1.
566 In this study, since the risk of developing thrombosis is expected to increase as travel time increases
567 by cumulative exposure to environmental risk factors, it was necessary to investigate whether the fluctuations
568 in the number of patients really reflect the periodicity by confirming the fluctuation of the percentage of onset
569 patients to the total number of passengers to examine whether the fluctuation reflects the increase or decrease
570 in the number of passengers. However, this confirmation could not be made because data on the total number

of passengers was not available. So, we focused on a method that suppressed the influence of the height of the wave and evaluated only curved shapes. Therefore, we decided to draw a correlogram that reduced wave height by the property of the correlation coefficient, which fluctuates only between -1 and 1.

However, Pearson's product-moment correlation coefficient has a weakness: it is easily affected by outliers. Also, as the progress of shifting the one side of the data string against the original data, their correspondence decreases. In other words, the number of data that can be used to calculate the correlation coefficient gradually decreases. This problem may cause considerable variation between the calculated correlation coefficients. Also, the thrombosis onset was recorded in 1-hour increments, and the length of the data was limited to 24 hours (24 data points). Therefore, instead of Pearson's product-moment correlation coefficient, we decided to create a correlogram using Spearman's rank correlation coefficient.

6. Analysis 2 (dataset: COVID-19)[33]

1) Dataset search and data review

c. Dataset search

To apply our idea to COVID-19 problems, one of the authors (KK) searched hyperbolic patterns using a search service Google (https://www.google.com/) provided by Google Inc., which allows displaying search results as "images." The search keyword was "COVID-19 AND Meta-analysis". In the case of displaying bubble charts instead of the error bars, the size of the bubble chart (inversely proportional to the length of the error bars) was converted in mind. Consequently, we selected a suspicious study reported by

590 Matsushita et al. (Matsushita, K. et al., *Glob Heart.* 2020;15(1):64.)[33] that included eight research papers in

591 Figure 5[59-66].

592

593 d. Data review

594 As in the case of Analysis 1, we reviewed to evaluate numerical accuracy and appropriateness from

595 the viewpoints of biomedicine. Since Matsushita et al.[33] originally made web Figure 5 and excluded 17

596 studies[35,67-82] from avoiding duplication of studies in Wuhan city in the making of Figure 5, we inspected both

597 of studies in Figure 5 (8 studies) and only in web Figure 5 (17 studies).

598 Based on the results shown below, considering the issue of comparability, we excluded the data

599 reported by Yuan et al.[65] and Wang L. et al[63]. Also, we re-calculated age difference using data reported by

600 Guan et al. [61] **(see Extended Data Fig. 1)**.

601 As a side note, the numbers assigned to each point in figure 3 were the same numbers described in

602 the original figure by Matsushita et al.[33], and the correspondence relationship is the following **(Fig. 3)**: **No.2**:

603 Cao et al. (Cao, J. et al., *Intensive Care Med.* 2020;46(5):851-853.)[59], **No.7**: Deng et al. (Deng, Y. et al., *Chin*

604 *Med J (Engl).* 2020;133(11):1261-1267.)[60], **No.8**: Guan et al. (Guan, W.J. et al., *N Engl J Med.*

605 2020;382(18):1708-1720.)[61], **No.19**: Wang D. et al. (Wang, D. et al., *JAMA.* 2020;323(11):1061-1069.)[62],

606 **No.20**: Wang L. et al. (Wang, L. et al., *J Infect.* 2020;80(6):639-645.)[63], **No.21**: Wu et al. (Wu, C. et al., *JAMA*

607 *Intern Med.* 2020;180(7):934-943.)[64], **No.23**: Yuan et al. (Yuan, M. et al., *PLoS One.* 2020;15(3):e0230548)[65],

608 **No.25**: Zhou et al. (Zhou, F. et al., *Lancet.* 2020;395(10229):1054-1062.)[66].

609

610 (i) No.8 Guan et al. (Guan, W.J. et al., *N Engl J Med.* 2020;382(18):1708-1720.)[61]

611 We found a matter of consideration in the data reported by Guan et al[61]. Initially, features of that

612 data differed from the other studies, which contained only cases reported from Wuhan city. In contrast, the

613 data reported by Guan et al.[61] contained cases outside of Wuhan city. Also, regarding the situation of the early

614 pandemic, there were concerns about the presence of patients who could not take appropriate medication,

615 especially in non-urban areas. Also, Matsushita et al.[33] did not use the data divided into the severe and non-

616 severe groups by Guan et al.[61] but used the data divided into yes and no by Guan et al.[61] using "Presence of

617 Primary Composite End Point", which means entry to the intensive care unit (ICU), use of mechanical

618 ventilation, or death.

619 Since Cao et al. (Wuhan University Zhongnan Hospital in Wuhan; affiliation of Dr Jianlei Cao:

620 Department of Cardiology)[59] and Wang et al. (Zhongnan Hospital of Wuhan University in Wuhan; affiliation

621 of Dawei Wang, MD: Department of Critical Care Medicine)[62] also used ICU admission as a criterion for

622 severe or non-severe, we examined the rate of severely ill patients and resulted in 21.4% (18/84) and 35.3%

623 (36/102), respectively. However, in the case of using the "Presence of Primary Composite End Point", the

624 percentage was only 6.5% (67/1032). Whereas, in the original categorisation by Guan et al.[61], the percentage

625 was 18.7% (173/926). Therefore, we prioritised the original classification of severe or non-severe by Guan et

626 al[61].

627

(ii) No. 9 Guo et al. (Guo et al. *JAMA Cardiol.* 2020;5(7):811- 818)[35] (only in eFigure5)

We read this paper carefully, a report from Wuhan city published in March 2020. Although this document may significantly influence the studies on COVID-19 (according to the JAMA Cardiology website, the article was cited more than 1,500 as of 20th September 2021), we found that misuse of linear regression analysis in Guo et al. on a figure (see Extended Data Fig. 8 & **Supplementary discussion 5: misuse of linear regression analysis**)[35].

Additionally, three subgroup patterns appeared in a figure reported by Guo et al., although they did not mention it. Precautionary, we considered whether the subgroups in the Guo et al.[35] affected the meta-analysis on the web Figure 5. The data in other studies allowed to be expected to have the same subgroups because the patient data described by Guo et al.[71] and other studies were reported from China (most of them were in Wuhan City).

(iii) No. 20 Wang L. et al. (Wang, D. et al., *JAMA.* 2020;323(11):1061-1069.)[63]

In confirming from the viewpoint of the biomedicine side, it was found that a significant matter of consideration on eligibility, patient population reported by Wang L. et al. was limited to over age 60[63]. The title was "Coronavirus disease 2019 in elderly patients: Characteristics and prognostic factors based on 4-week follow-up", and Matsushita et al. [33] had to pay attention to the word "elderly".

(iv) No.23 Yuan M. et al. (Yuan M. et al., *PLoS One.* 2020;15(3):e0230548.)[65]

In confirming the accuracy of values, we found a mixture of values derived from different calculation types in Figure 5: Odds Ratio (OR), hazard ratio, and a value derived from the imputation of 0.5 for the zero cells in the cross table. The zero cells appeared in the study reported by Yuan et al[65]. Yuan M. et al. studied 27 patients who confirmed novel coronavirus infected pneumonia (NCIP) during the early phase of the pandemic to evaluate radiologic characteristics[65]. In other words, the difficulty of patient enrollment might cause a small sample size, which seemed to be a concern from the viewpoint of comparability (c.f., Guan W. et al., n=1099[61]; Zhou F. et al., n=191[66]; Wang D. et al., n=138[62]; Wu C. et al. n=201[64]; Cao J. et al., n=102[59]; Deng Y. et al., n=225[60]).

(v) The term "Cardiovascular disease (CVD)."

There was an inconsistency in the studies on "Cardiovascular disease (CVD)." For example, vascular diseases such as arrhythmia and arteriosclerosis are also classified as CVD, but in the studies reported by Guan et al.[61] and Zhou et al.[66], the term "Coronary heart disease" was used. Also, "Cardiac disease" was used by Yuan et al.[65], "Heart disease" was used by Deng et al.[60], and "Cardiovascular disease" was used by Wang L et al[63].

2) Regression analysis

Considering the problem of comparability, we re-calculated OR and visually grouped it into two hyperbolic patterns. In the case of S-shaped curve fitting, since there were many unknown coefficients for the number of data (3 unknown coefficients of K_1, K_2, and M), the regression analysis was performed after setting the zero point value. In the fitting of upper and lower curves, since there were many unknown coefficients (K_1, K_2, M, a, b, c), we firstly obtained the coefficient of M (see equation (1)) by the curve fitting of the S-shaped curve, and then performed curve fitting of parabolas. After substituting M for x value of apex in equation (4) (see equations (4) & (5)), regression analysis was performed on the data in the middle row of Figure 3 **(Fig. 3, d-f)**. Finally, the S-shaped curve and the parabola were merged **(Fig. 3, g-i)**.

3) Calculation of weighted average

In earlier days group, the median age and the number of cases are tabulated by severe and non-severe cases as follows. Guan W. et al. (severe n=173 [age: 52] vs non-severe n=926 [age: 45])[61], Zhou F. et al. (non-survival n=54 [age: 69] vs survival n=137 [age: 52])[66], Wang D. et al. (ICU n=36 [age: 66] vs non-ICU n=102 [age: 51])[62], Wu C. et al. (ARDS n=84 [age: 58.5] vs non-ARDS n=117 [age: 48])[64], and whole of earlier days group (severe n = 347 vs non-severe n = 1282).

The weighted average of severe and non-severe in the earlier days group was calculated from these values by the following formulas. In the earlier days group, the weighted average of severe and non-severe were 57.7 and 46.5, respectively.

682

683 $$Number\ of\ patients\ in\ earlier\ days\ group\ (severe) = 173 + 54 + 36 + 84 = \mathbf{347}$$

684 $$Weighted\ mean\ of\ earlier\ days\ group\ (severe) = \frac{173}{\mathbf{347}} \times 52 + \frac{54}{\mathbf{347}} \times 69 + \frac{36}{\mathbf{347}} \times 66 + \frac{84}{\mathbf{347}} \times 58.5$$

685 $$\cong 57.7$$

686

687 $$Number\ of\ patients\ in\ earlier\ days\ group(non - severe) = 926 + 137 + 102 + 117 = \mathbf{1282}$$

688 $$Weighted\ mean\ of\ earlier\ days\ group\ (non - severe)$$

689 $$= \frac{926}{\mathbf{1282}} \times 45 + \frac{137}{\mathbf{1282}} \times 52 + \frac{102}{\mathbf{1282}} \times 51 + \frac{117}{\mathbf{1282}} \times 48 \cong 46.5$$

690

691 In later days group, the median age and the number of cases are tabulated by severe and non-severe

692 cases as follows. Cao J. et al. (ICU n=18 [age: 66] vs non-ICU n=84 [age: 31])[59], Deng Y. et al. (Death n=109

693 [age: 69] vs survival n=116 [age: 48])[60], and whole of later days group (severe n = 127 vs non-severe n =

694 200).

695 The weighted average of severe and non-severe in the late date group was calculated from these

696 values by the following formulas. In the late date group, the weighted average of severe and non-severe were

697 68.6 years and 40.9, respectively.

698

699 $$Number\ of\ patients\ in\ late\ date\ group\ (severe) = 18 + 109 = \mathbf{127}$$

700 $$Weighted\ mean\ of\ late\ date\ group\ (severe) = \frac{18}{\mathbf{127}} \times 66 + \frac{109}{\mathbf{127}} \times 69 \cong 68.6$$

$$Number\ of\ patients\ in\ late\ date\ group\ (non-severe) = 84 + 116 = \mathbf{200}$$

$$Weighted\ mean\ of\ late\ date\ group\ (non-severe) = \frac{84}{\mathbf{200}} \times 31 + \frac{116}{\mathbf{200}} \times 48 \cong 40.9$$

4) Additional analysis: Regression analysis on the parabolic cylinder

One of the authors (KK) found a way to fit an appropriate curve to the data reported by Guo et al., performing trial and error with his mathematical intuition **(Fig. 4)**. Firstly, he calculated the centre of gravity of the data by each subgroup cluster (centre of gravity: the average of the values on the horizontal axis x and the average of the values on the vertical axis y). Second, he obtained equations of three straight lines passing through the origin and centres of gravity. Thirdly, he obtained the equation of a straight line passing through each centre of gravity and intersecting the straight lines obtained above. Fourthly, he re-set new origin as each centre of gravity and regarded the above two crossed lines as a small cartesian coordinate system. Finally, he applied parabola fitting with Excel® in each new cartesian coordinate system. In this curve fitting, he used the data of distance between each data point and the straight line obtained secondary, and the data of distance between each data point and the straight line obtained firstly (see "distance from a point to a line" in a high school textbook).

5) Making example data

To explain the misuse of linear regression analysis in Guo et al.[35], we made the following data to show the example. It allows being used in R by copying and pasting the following.

```
Value_X<-
c(0.04 ,0.08 ,0.12 ,0.16 ,0.2 ,0.24 ,0.28 ,0.32 ,0.36 ,0.4 ,0.44 ,0.48 ,0.52 ,0.56 ,0.6 ,0.64 ,0.68 ,0.72 ,0.76 ,0.8 ,0
.84 ,0.88 ,0.92 ,0.96 ,1 ,1.04 ,1.08 ,1.12 ,1.16 ,1.2 ,1.24 ,1.28 ,1.32 ,1.36 ,1.4 ,1.44 ,1.48 ,1.52 ,1.56 ,1.6 ,1.64 ,
1.68 ,1.72 ,1.76 ,1.8 ,1.84 ,1.88 ,1.92 ,1.96 ,2 ,2.04 ,2.08 ,2.12 ,2.16 ,2.2 ,2.24 ,2.28 ,2.32 ,2.36 ,2.4 ,2.44 ,2.48
,2.52 ,2.56 ,2.6 ,2.64 ,2.68 ,2.72 ,2.76 ,2.8 ,2.84 ,2.88 ,2.92 ,2.96 ,3 ,3.04 ,3.08 ,3.12 ,3.16 ,3.2 ,3.24 ,3.28 ,3.32
,3.36 ,3.4 ,3.44 ,3.48 ,3.52 ,3.56 ,3.6 ,3.64 ,3.68 ,3.72 ,3.76 ,3.8 ,3.84 ,3.88 ,3.92 ,3.96 ,4)

Value_Y<-
c(2.01742 ,2.02749 ,2.04454 ,2.02009 ,2.03445 ,2.04749 ,2.03641 ,1.99047 ,1.98671 ,2.06711 ,2.09772 ,2.005
39 ,1.86985 ,2.01679 ,2.12183 ,1.94453 ,1.86497 ,1.87444 ,2.09483 ,1.91073 ,1.69244 ,1.70968 ,1.81376 ,2.0
4219 ,1.69059 ,1.75939 ,1.95321 ,1.8417 ,1.58169 ,1.75585 ,1.73497 ,1.47847 ,1.9115 ,1.44962 ,1.85063 ,1.3
2298 ,1.28437 ,1.74621 ,1.27232 ,1.32763 ,1.575 ,1.56609 ,1.5933 ,1.76707 ,1.11264 ,1.06188 ,1.40139 ,0.94
084 ,1.0756 ,1.38507 ,1.33408 ,1.54375 ,1.60257 ,1.02029 ,0.98612 ,1.79094 ,0.97916 ,0.81212 ,1.1484 ,1.51
68 ,1.70236 ,1.38945 ,1.69072 ,1.75042 ,1.67571 ,1.38623 ,1.81503 ,1.80665 ,1.41073 ,2.3175 ,2.24852 ,1.75
95 ,2.81818 ,1.93654 ,2.36998 ,2.0987 ,2.19539 ,2.44747 ,2.57255 ,3.24637 ,2.78881 ,3.51638 ,2.68107 ,2.87
259 ,4.3749 ,3.13393 ,3.92099 ,4.1223 ,3.78584 ,4.9666 ,5.4888 ,5.70712 ,4.84752 ,5.1409 ,6.31637 ,5.53198
,6.89257 ,7.86387 ,7.98237 ,8.64705)
```

7. Statement of our intention for data review results

To clarify our stance, we mention this statement of intention for results. In this article, we pointed out many overlooking and errors. However, we have no intention to attack previous works because our analysis results owing to their original works, including original research articles, reported valuable data and articles of meta-analysis synthesised valuable datasets. Since just a scientist had better reconfirm the previous studies with no preconception with being grateful to the researchers of those studies, we carefully reviewed the data reported by previous studies. We highly respect previous works, which have the intention to solve medical issues, although some articles contained technical errors.

748

749 **Methods references**

750 51 Belcaro, G., Geroulakos, G., Nicolaides, A. N., Myers, K. A. & Winford, M. Venous
751 thromboembolism from air travel: the LONFLIT study. *Angiology* **52**, 369-374,
752 doi:10.1177/000331970105200601 (2001).
753 52 Gajic, O. *et al.* Long-haul air travel before major surgery: a prescription for thromboembolism?
754 *Mayo Clin Proc* **80**, 728-731, doi:10.1016/S0025-6196(11)61525-5 (2005).
755 53 Hughes, R. J. *et al.* Frequency of venous thromboembolism in low to moderate risk long distance air
756 travellers: the New Zealand Air Traveller's Thrombosis (NZATT) study. *Lancet* **362**, 2039-2044,
757 doi:10.1016/s0140-6736(03)15097-0 (2003).
758 54 Jacobson, B. F. *et al.* The BEST study--a prospective study to compare business class versus
759 economy class air travel as a cause of thrombosis. *S Afr Med J* **93**, 522-528 (2003).
760 55 Lapostolle, F. *et al.* Severe pulmonary embolism associated with air travel. *N Engl J Med* **345**, 779-
761 783, doi:10.1056/NEJMoa010378 (2001).
762 56 Pérez-Rodríguez, E. *et al.* Incidence of air travel-related pulmonary embolism at the Madrid-Barajas
763 airport. *Arch Intern Med* **163**, 2766-2770, doi:10.1001/archinte.163.22.2766 (2003).
764 57 Schwarz, T. *et al.* Deep vein and isolated calf muscle vein thrombosis following long-haul flights:
765 pilot study. *Blood Coagul Fibrinolysis* **13**, 755-757, doi:10.1097/00001721-200212000-00013
766 (2002).

58 Schwarz, T. *et al.* Venous thrombosis after long-haul flights. *Arch Intern Med* **163**, 2759-2764, doi:10.1001/archinte.163.22.2759 (2003).

59 Cao, J. *et al.* Clinical features and short-term outcomes of 18 patients with corona virus disease 2019 in intensive care unit. *Intensive Care Med* **46**, 851-853, doi:10.1007/s00134-020-05987-7 (2020).

60 Deng, Y. *et al.* Clinical characteristics of fatal and recovered cases of coronavirus disease 2019 in Wuhan, China: a retrospective study. *Chin Med J (Engl)* **133**, 1261-1267, doi:10.1097/CM9.0000000000000824 (2020).

61 Guan, W. J. *et al.* Clinical Characteristics of Coronavirus Disease 2019 in China. *N Engl J Med* **382**, 1708-1720, doi:10.1056/NEJMoa2002032 (2020).

62 Wang, D. *et al.* Clinical Characteristics of 138 Hospitalized Patients With 2019 Novel Coronavirus-Infected Pneumonia in Wuhan, China. *JAMA* **323**, 1061-1069, doi:10.1001/jama.2020.1585 (2020).

63 Wang, L. *et al.* Coronavirus disease 2019 in elderly patients: Characteristics and prognostic factors based on 4-week follow-up. *J Infect* **80**, 639-645, doi:10.1016/j.jinf.2020.03.019 (2020).

64 Wu, C. *et al.* Risk Factors Associated With Acute Respiratory Distress Syndrome and Death in Patients With Coronavirus Disease 2019 Pneumonia in Wuhan, China. *JAMA Intern Med* **180**, 934-943, doi:10.1001/jamainternmed.2020.0994 (2020).

784 65 Yuan, M., Yin, W., Tao, Z., Tan, W. & Hu, Y. Association of radiologic findings with mortality of
785 patients infected with 2019 novel coronavirus in Wuhan, China. *PLoS One* **15**, e0230548,
786 doi:10.1371/journal.pone.0230548 (2020).
787 66 Zhou, F. *et al.* Clinical course and risk factors for mortality of adult inpatients with COVID-19 in
788 Wuhan, China: a retrospective cohort study. *Lancet* **395**, 1054-1062, doi:10.1016/S0140-
789 6736(20)30566-3 (2020).
790 67 Bhatraju, P. K. *et al.* Covid-19 in Critically Ill Patients in the Seattle Region - Case Series. *N Engl J*
791 *Med* **382**, 2012-2022, doi:10.1056/NEJMoa2004500 (2020).
792 68 CDC COVID-19 Response Team. Preliminary Estimates of the Prevalence of Selected Underlying
793 Health Conditions Among Patients with Coronavirus Disease 2019 - United States, February 12-
794 March 28, 2020. *MMWR Morb Mortal Wkly Rep* **69**, 382-386, doi:10.15585/mmwr.mm6913e2
795 (2020).
796 69 CDC COVID-19 Response Team. Severe Outcomes Among Patients with Coronavirus Disease
797 2019 (COVID-19) - United States, February 12-March 16, 2020. *MMWR Morb Mortal Wkly Rep*
798 **69**, 343-346, doi:10.15585/mmwr.mm6912e2 (2020).
799 70 Chen, J. *et al.* Clinical progression of patients with COVID-19 in Shanghai, China. *J Infect* **80**, e1-
800 e6, doi:10.1016/j.jinf.2020.03.004 (2020).
801 71 Chen, T. *et al.* Clinical characteristics of 113 deceased patients with coronavirus disease 2019:
802 retrospective study. *BMJ* **368**, m1091, doi:10.1136/bmj.m1091 (2020).

803 72 Cheng, Y. *et al.* Kidney disease is associated with in-hospital death of patients with COVID-19.
804 *Kidney Int* **97**, 829-838, doi:10.1016/j.kint.2020.03.005 (2020).
805 73 Huang, C. *et al.* Clinical features of patients infected with 2019 novel coronavirus in Wuhan, China.
806 *Lancet* **395**, 497-506, doi:10.1016/S0140-6736(20)30183-5 (2020).
807 74 Lian, J. *et al.* Analysis of Epidemiological and Clinical Features in Older Patients With Coronavirus
808 Disease 2019 (COVID-19) Outside Wuhan. *Clin Infect Dis* **71**, 740-747, doi:10.1093/cid/ciaa242
809 (2020).
810 75 Liang, W. *et al.* Cancer patients in SARS-CoV-2 infection: a nationwide analysis in China. *Lancet*
811 *Oncol* **21**, 335-337, doi:10.1016/S1470-2045(20)30096-6 (2020).
812 76 Onder, G., Rezza, G. & Brusaferro, S. Case-Fatality Rate and Characteristics of Patients Dying in
813 Relation to COVID-19 in Italy. *JAMA* **323**, 1775-1776, doi:10.1001/jama.2020.4683 (2020).
814 77 Ruan, Q., Yang, K., Wang, W., Jiang, L. & Song, J. Clinical predictors of mortality due to COVID-
815 19 based on an analysis of data of 150 patients from Wuhan, China. *Intensive Care Med* **46**, 846-
816 848, doi:10.1007/s00134-020-05991-x (2020).
817 78 Shi, S. *et al.* Association of Cardiac Injury With Mortality in Hospitalized Patients With COVID-19
818 in Wuhan, China. *JAMA Cardiol* **5**, 802-810, doi:10.1001/jamacardio.2020.0950 (2020).
819 79 Tang, N., Li, D., Wang, X. & Sun, Z. Abnormal coagulation parameters are associated with poor
820 prognosis in patients with novel coronavirus pneumonia. *J Thromb Haemost* **18**, 844-847,
821 doi:10.1111/jth.14768 (2020).

80 The Novel Coronavirus Pneumonia Emergency Response Epidemiology Team. The Epidemiological Characteristics of an Outbreak of 2019 Novel Coronavirus Diseases (COVID-19) — China, 2020. *China CDC Weekly* **2**, 113-122, doi:https://doi.org/10.46234/ccdcw2020.032 (2020).

81 Yang, X. *et al.* Clinical course and outcomes of critically ill patients with SARS-CoV-2 pneumonia in Wuhan, China: a single-centered, retrospective, observational study. *Lancet Respir Med* **8**, 475-481, doi:10.1016/S2213-2600(20)30079-5 (2020).

82 Zhang, L. *et al.* Clinical characteristics of COVID-19-infected cancer patients: a retrospective case study in three hospitals within Wuhan, China. *Ann Oncol* **31**, 894-901, doi:10.1016/j.annonc.2020.03.296 (2020).

83 Reyes, N. L., Beckman, M. G. & Abe, K. in *CDC Yellow Book 2020 Health Information for International Travel* (eds Centers for Disease Control and Prevention (CDC), G. W. Brunette, & J. B. Nemhauser) Ch. 8, (Oxford University Press, 2019).

84 Kushner, A., West, W. P. & Pillarisetty, L. S. (2021).

85 Thachil, J. *et al.* ISTH interim guidance on recognition and management of coagulopathy in COVID-19. *J Thromb Haemost* **18**, 1023-1026, doi:10.1111/jth.14810 (2020).

86 Sugawa, S. Significance of Screening the General Population for Potential Cardiovascular Diseases with a Combination Assay of B-type Natriuretic Peptide and High Sensitive Troponin I. *J Med Diagn Meth* **6** (2017).

Acknowledgements

One of the authors, Keiichiro Kimoto, appreciates the kindful encouragement of Hideo Yoshioka, MEcon., who is in charge of the Data Strategy Research Institute representative.

Competing interest declaration

Keiichiro Kimoto has been in charge of external advisor for Data Strategy Research Institute but reserved no financial support for this study. Except for this, the authors have no conflicts of interest and have no financial disclosures that should be disclosed.

Author contributions

Keiichiro Kimoto takes responsibility for this research, making study concepts, data analysis, interpretation of analysis results, and drafting the manuscript. Dr. Yamakuchi contributed to interpreting analysis results, manuscript drafting, supervision and administrative role. Dr. Takenouchi contributed to the supervision. Dr. Hashiguchi contributed to the study concept, interpretation of analysis results, manuscript drafting, supervision, and administrative role.

Additional information

This article has supplementary information that contains supplementary discussions.

860

861 **Data availability statement**

862 We analyzed clinical data published by other studies (third parties). Used data is identified by

863 indicated information of citation (reference numbers and list of references). The corresponding author

864 responds to inquiries in the case of measured values from published figures requested by reviewers or readers.

865

866 **Code availability statement**

867 Correspondence author (KK) can respond to inquiries for the corresponding author's email address

868 on offering the Python source code and spreadsheet software files for statistical analysis.

869

870

871 **Figures & figure legends**

872 **Fig. 1**

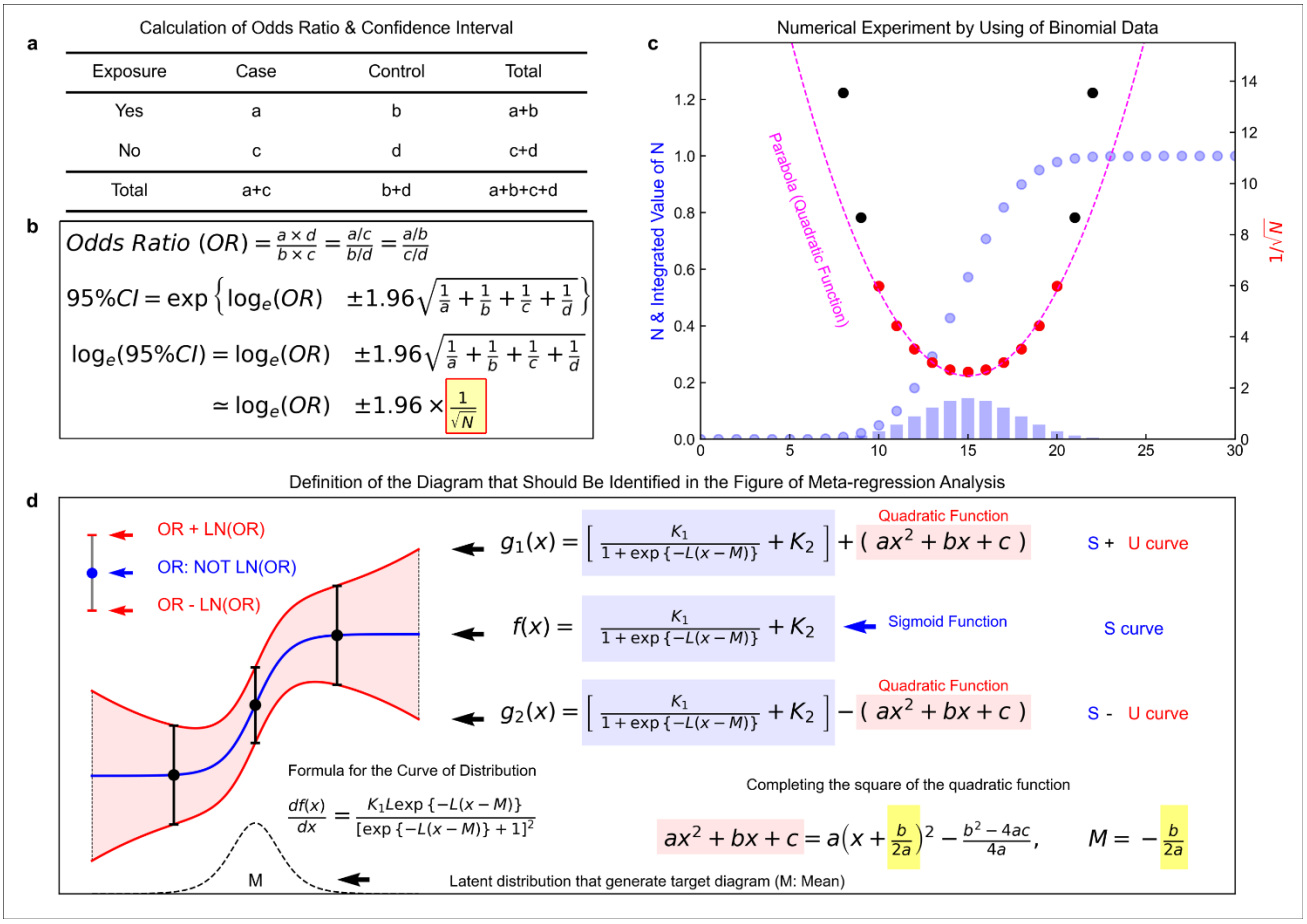

873

874 **Fig. 1 | A hyperbolic shape formed by confidence limits. a,** A two-way cross-tabulation (contingency table)

875 for calculating an odds ratio (OR). **b**, Calculation of OR and its 95% confidence interval. **c**, Histogram of the

876 data following a binomial distribution and a plot of the inverse values of the square roots. **d**, The mathematical

877 formulas for the hyperbolic shape. Note that the OR is not logarithmic, and only the length of the error bar is

878 logarithmic (see the upper left position of panel d).

879

Fig. 2

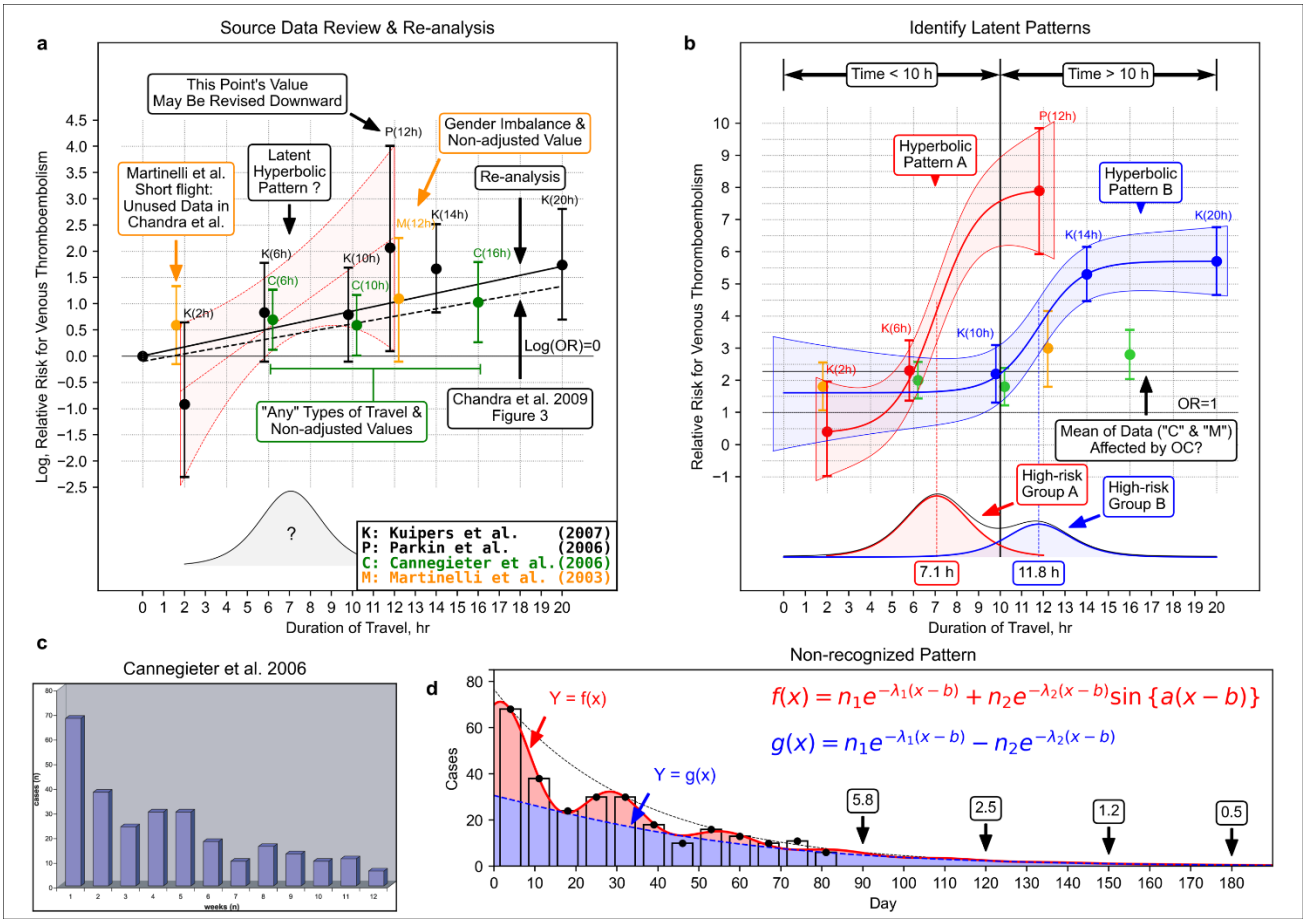

Fig. 2 | Re-analysis based on the proposed ideas. a, Data review and meta-regression analysis using the same method as Chandra et al. *Ann Intern Med.* 2009; 151(3):180-190. Figure 3[7]. We added information from original studies and our hypothesis to the previously published form, such as latent distribution. The original figure has been shown on the American College of Physicians website, which links to PubMed® (https://pubmed.ncbi.nlm.nih.gov/19581633/). From Chandra D, Parisini E, Mozaffarian D. Meta-analysis: travel and risk for venous thromboembolism. Ann Intern Med. 2009 Aug 4;151(3):180-90. doi: 10.7326/0003-4819-151-3-200908040-00129. Epub 2009 Jul 6. © 2009 American College of Physicians. Adapted with

permission. **b**, grouping the data and hyperbolic shape fitting. **c**, Onsets of thrombosis after travel reported by Cannegieter et al[25]. This figure was re-used and re-drawn from Cannegieter et al. Travel-related venous thrombosis: results from a large population-based case-control study (MEGA study). *PLoS Med.* 2006; 3(8):e307. Figure 1. https://www.ncbi.nlm.nih.gov/labs/pmc/articles/PMC1551914/figure/pmed-0030307-g001/ Copyright © 2006 Cannegieter et al. Creative Commons Attribution License. In 2006, the Creative Commons Attribution 2.0 Generic, License was available. https://creativecommons.org/licenses/by/2.0/ **d**, Applying the damped wave function to the data shown in panel c. We decided that the data from Martinelli et al.[23] and Cannegieter et al.[25] should be excluded, and the odds ratio from Parkin et al.[24] may decrease (see Methods). At 2 hours point, Chandra et al.[7] did not use available data (panel a). On the original regression line, Chandra et al.[7] might conduct a meta-regression analysis reversing the front head and the front side of the cross-tabulation. Compering panels c and d helps us understand that using a three-dimensional graph disrupts our recognition.

904

905 **Fig. 3**

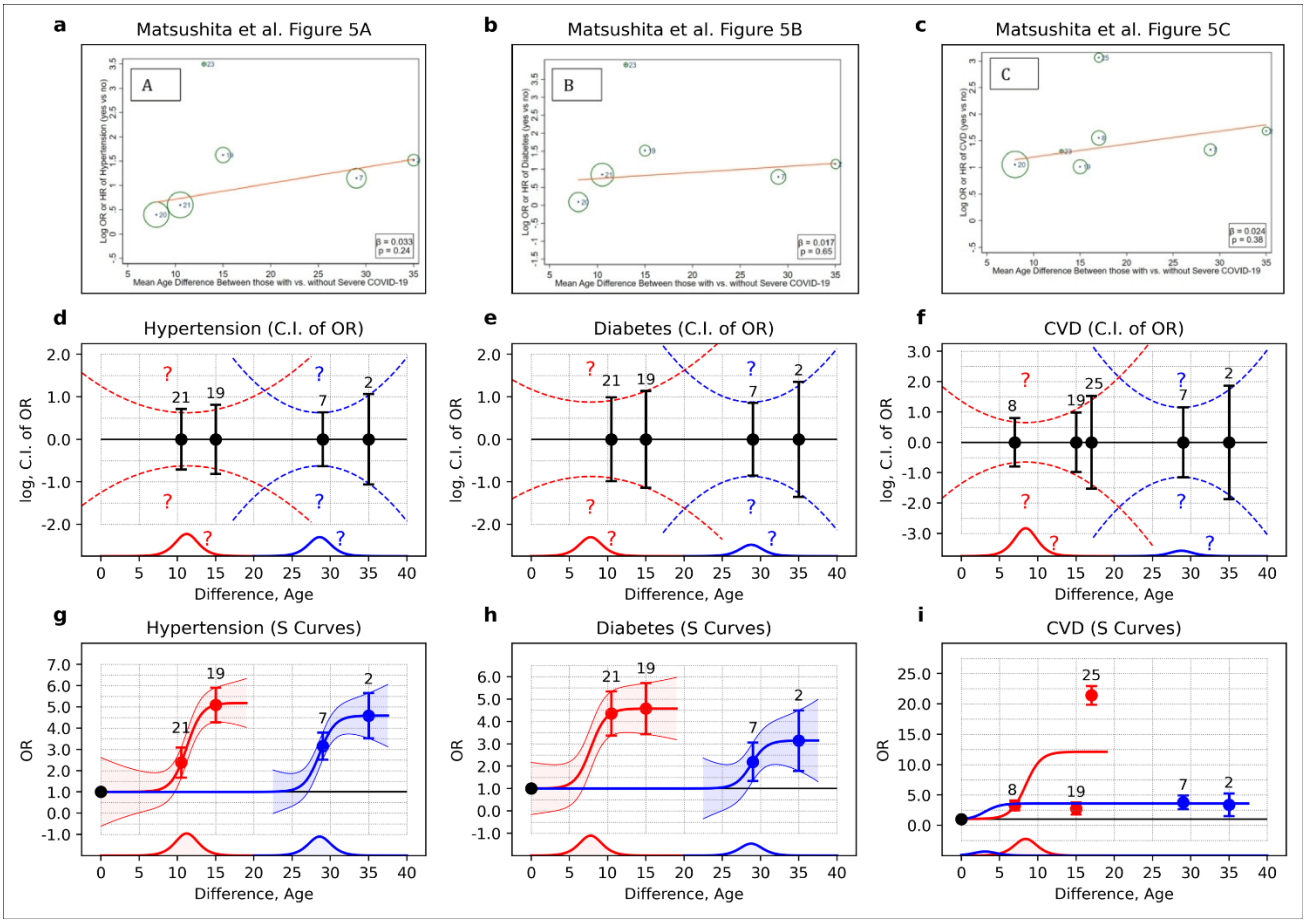

906

907 **Fig. 3 | Hyperbolic shapes found in the figure reported by Matsushita et al[33]. a**, A figure shows the

908 relationship between the severe and non-severe groups reported by Matsushita et al.[33], which shows age

909 difference on the horizontal axis and odds ratio (OR) or hazard ratio of hypertension on the vertical axis. To

910 evaluate potential confounding for relative risk by age, Matsushita et al. conducted meta-regression analyses

911 based on the assumption that there was the possibility of confounding by age in the case that the study with a

912 larger age difference has a higher relative risk[33]. **b**, Diabetes. **c**, Cardiovascular disease (CVD). **d-f**,

913 Comparisons of error bars, which show 95% confidence interval (C.I.) s. It corresponds to the upper figure. **g-**

914 **i**, Hyperbolic patterns were fitted to the OR and the 95% confidence limit of the OR. In the panel i, a
915 hyperbolic shape could not be fitted due to the considerable data variation, likely due to the inconsistency of
916 the term "CVD" (see Methods). The numbers marked to each point are the same as the numbers shown in the
917 original figure. The sources of each data are shown in Methods. This figure was re-used from Matsushita et al.
918 *Glob Heart.* 2020; 15(1):64. Figure 5.
919 https://www.ncbi.nlm.nih.gov/labs/pmc/articles/PMC7546112/figure/F5/

922
923

924

925 **Fig. 4**

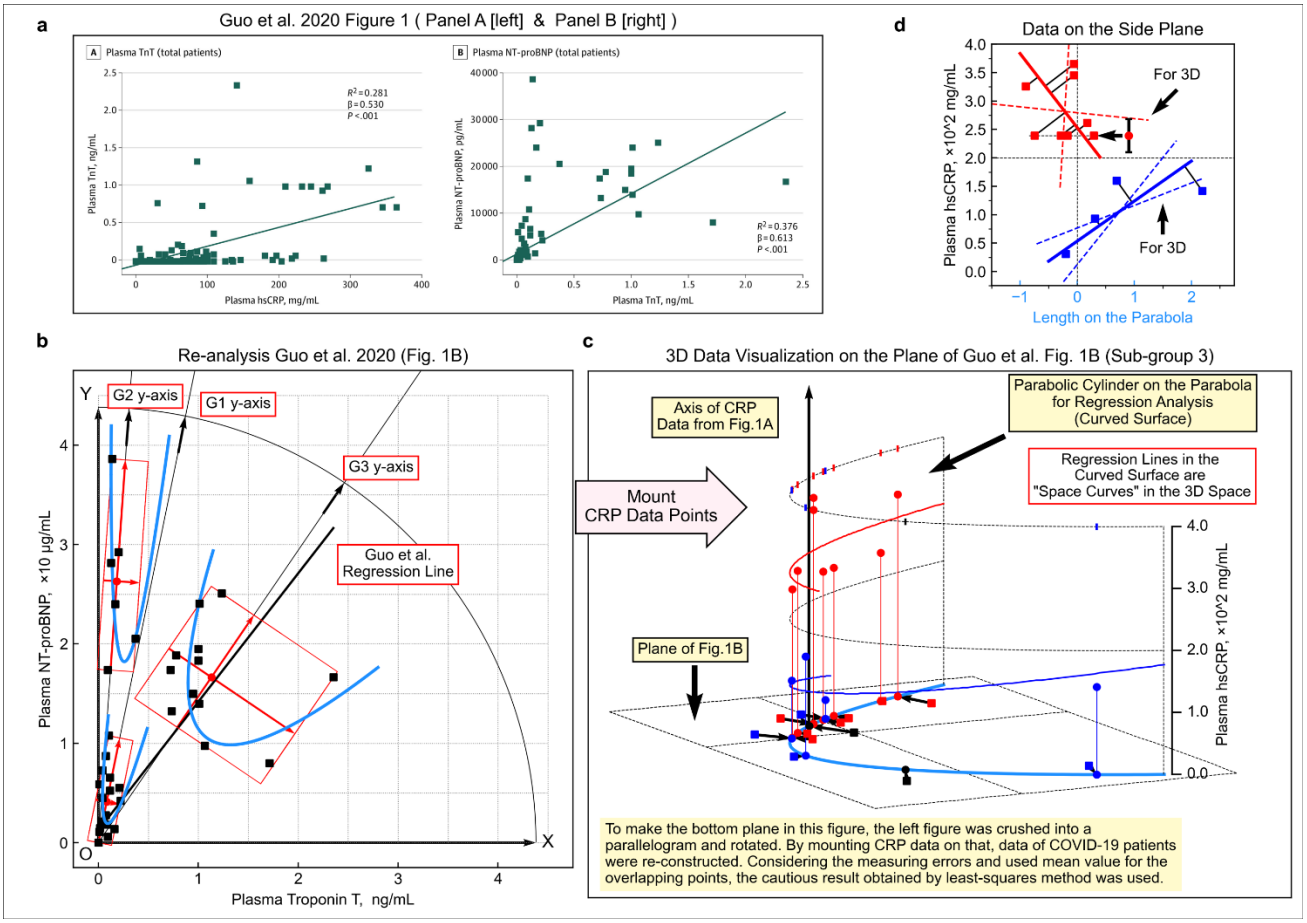

926

927 **Fig. 4 | Parabola shape patterns in the figure by Guo et al[35]. a**, Relationship between high sensitive C-

928 reactive protein (hsCRP) and cardiac troponin T (TnT) in COVID-19 patients (left) and relationship between

929 cardiac troponin T (TnT) and N-terminal pro-brain natriuretic peptide (NT-proBNP) (right). **b**, Data points

930 from the right side of the panel a and fitting parabola. **c**, Three-dimensional data visualisation was constructed

931 by mounting the value of hsCRP onto panel b. **d**, Linear regression analysis on the side surface of the

932 parabolic cylinder in panel c. The points were replaced with their average if the values could not be

933 determined due to overlapping (the points indicated by the left-pointing arrow and the error bar, which are the

934 average and the range of values, respectively). Panel a was re-used from Guo T et al. *JAMA Cardiol.* 2020;

935 5(7):811-818. Figure 1 https://www.ncbi.nlm.nih.gov/labs/pmc/articles/PMC7101506/figure/hoi200026f1/

936 Copyright © 2020 Guo T et al. JAMA Cardiology. Creative Commons Attribution License (CC-BY).

937 https://creativecommons.org/licenses/by/4.0/

938

939

940 **Extended data figures & figure legends**

941 **Extended Data Fig. 1**

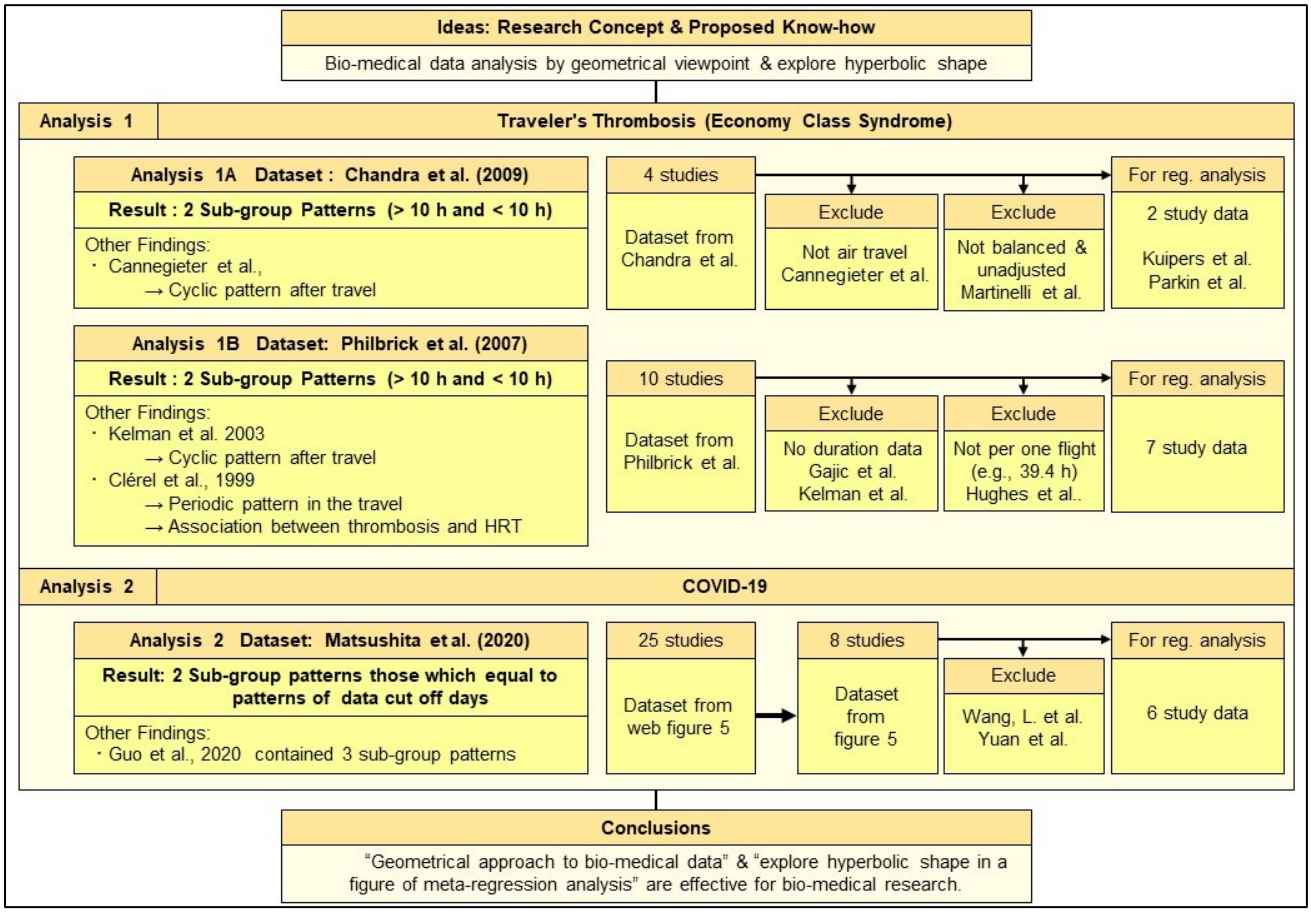

942

943

944 **Extended Data Fig. 1 | Overall framework of this study.** We applied our concept to traveller's thrombosis

945 and COVID-19. These were similar in research history (see Supplementary discussion 1: history of traveller's

946 thrombosis & Supplementary discussion 2: research situations of COVID-19 related thrombosis). In the case

947 of traveller's thrombosis, we analysed a dataset collected by Chandra et al. and Philbrick et al[4,7]. In the case of

948 COVID-19, we analysed a dataset collected by Matsushita et al[7]. Flow charts show data accept or reject flows.

949 Since duplicating data, Matsushita et al. selected only eight studies data (25 studies included in initial web Figure

950 5)[33].

951

952

953 **Extended Data Fig. 2**

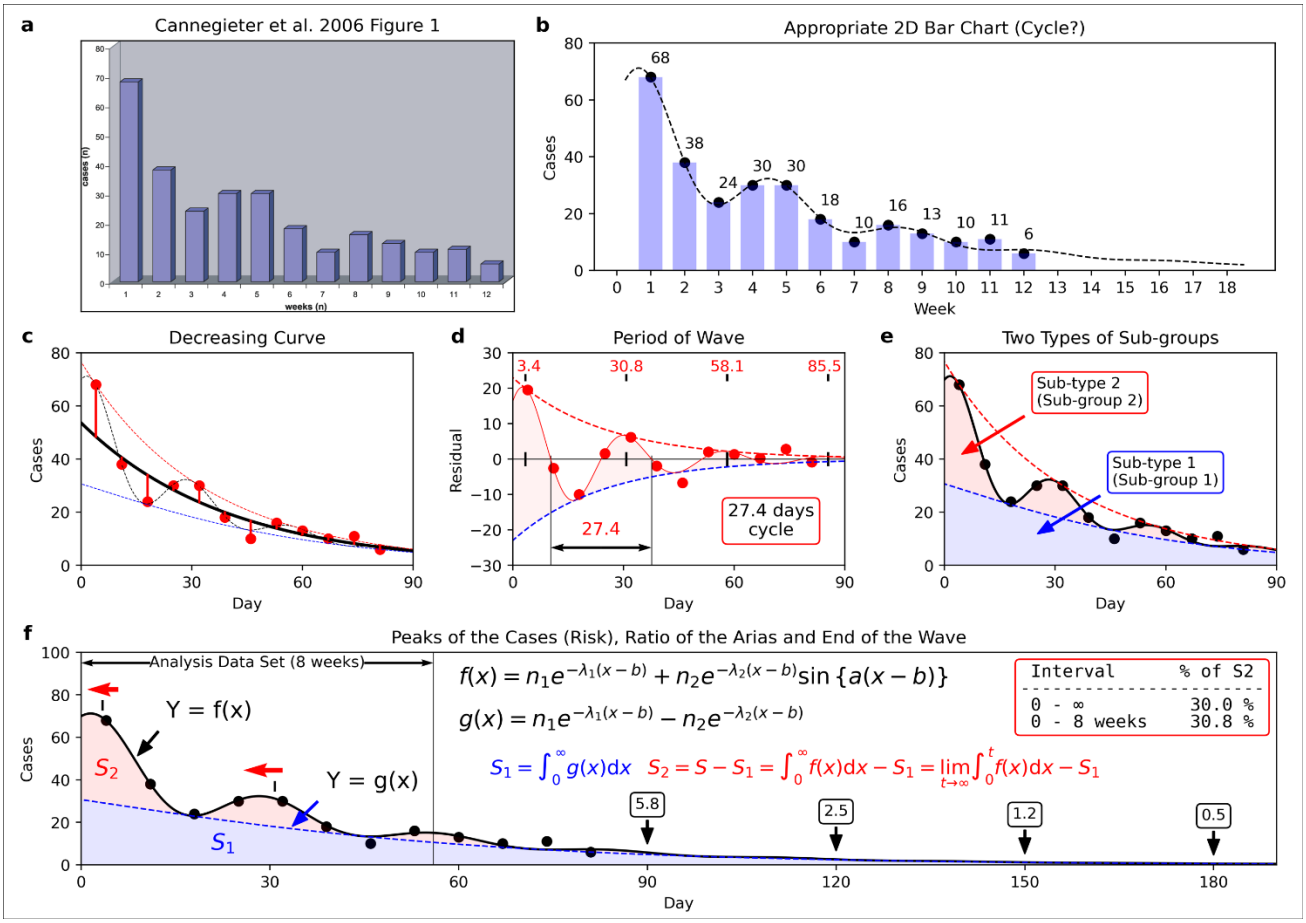

954

955 **Extended Data Fig. 2 | Unrecognised cyclic pattern of thrombosis onset after travel[25]. a**, A bar graph

956 showing the relationship between weeks after travel and the number of thrombosis onset in a figure reported

957 by Cannegieter et al[25]. **b**, Re-expressing as a two-dimensional bar graph avoiding the three-dimensional

958 representation. **c**, Applying a damped wave by non-linear regression analysis. **d**, Extraction of damped wave

959 part by subtracting the monotonic decrease function. **e**, Dividing into 2 sub-group areas by the envelopes of

960 the damped wave that touch the lower parts of the wave. **f**, Enlarged and added explanation of the ratio of the

961 area. Cannegieter et al.[25] used the data up to week eight, and the ratio of subgroup 2 to the total number of

962 patients (ratio of S_2 to the area of $S_1 + S_2$) was 30.0%. In the integration for the infinite interval, it was 30.8%.

963 Peak shifts of the wave (peak position of the wave shifted from the original to the other) appeared when

964 comparing panels d and f due to putting by regression curve located in the centre. Panel a was re-used from

965 Cannegieter et al. *PLoS Med.* 2006; 3(8):e307. Figure 1.

966 https://www.ncbi.nlm.nih.gov/labs/pmc/articles/PMC1551914/figure/pmed-0030307-g001/

967

968

969

970

971

972 **Extended Data Fig. 3**

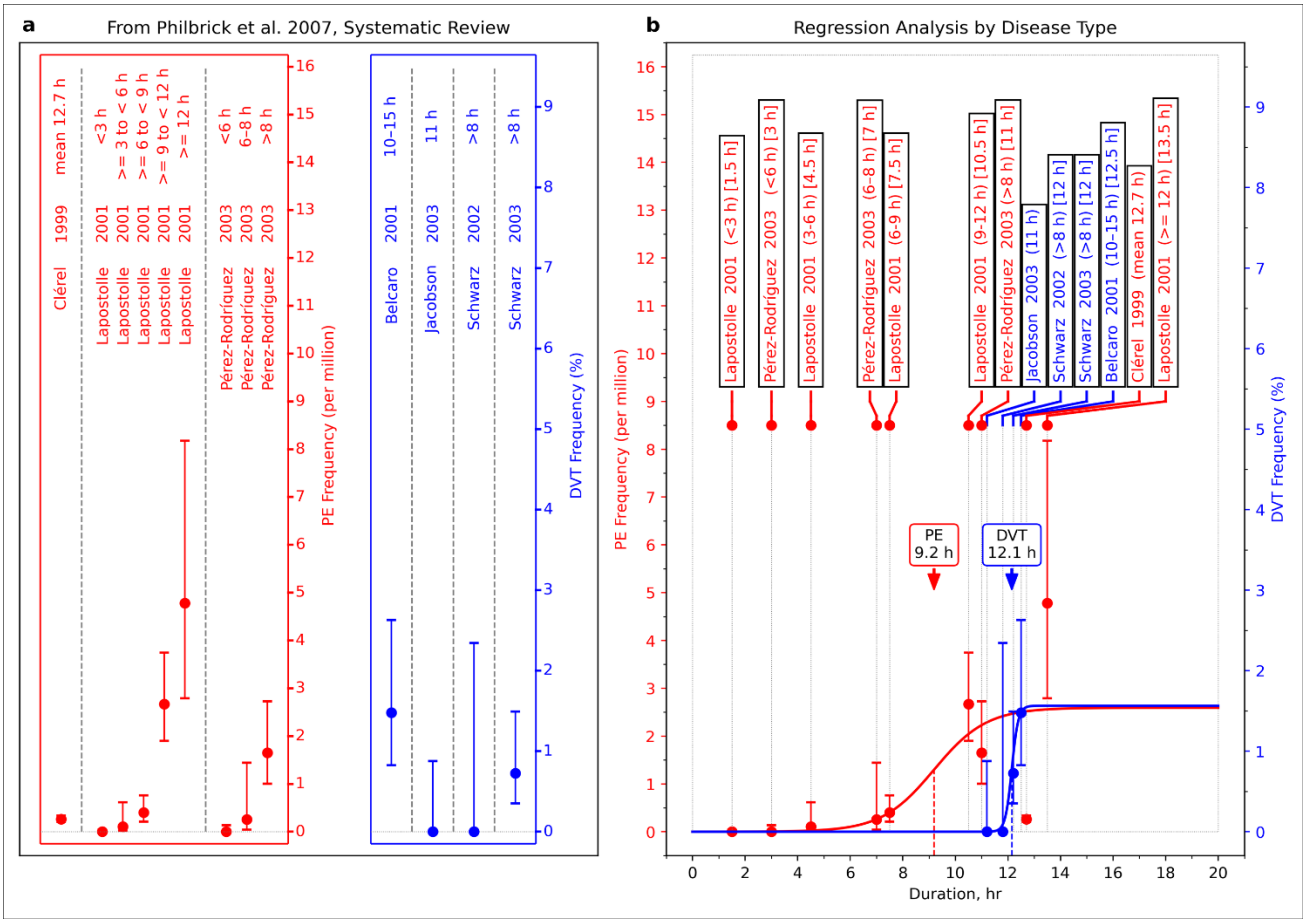

973

974 **Extended Data Fig. 3 | Curve fitting to the dataset reported by Philbrick et al[4]. a**, data stratification by

975 Pulmonary Embolism (PE) and Deep Vein Thrombosis (DVT). **b**, Application of S-shaped curve by

976 regression analysis to the stratified data. The value in the bracket (panel b) is the point of time converted from

977 the time category (see Methods). Philbrick et al.[4] reported the result of a systematic review with a table (list).

978 In contrast, this visualising allows us to extract latent information.

979

980

981 **Extended Data Fig. 4**

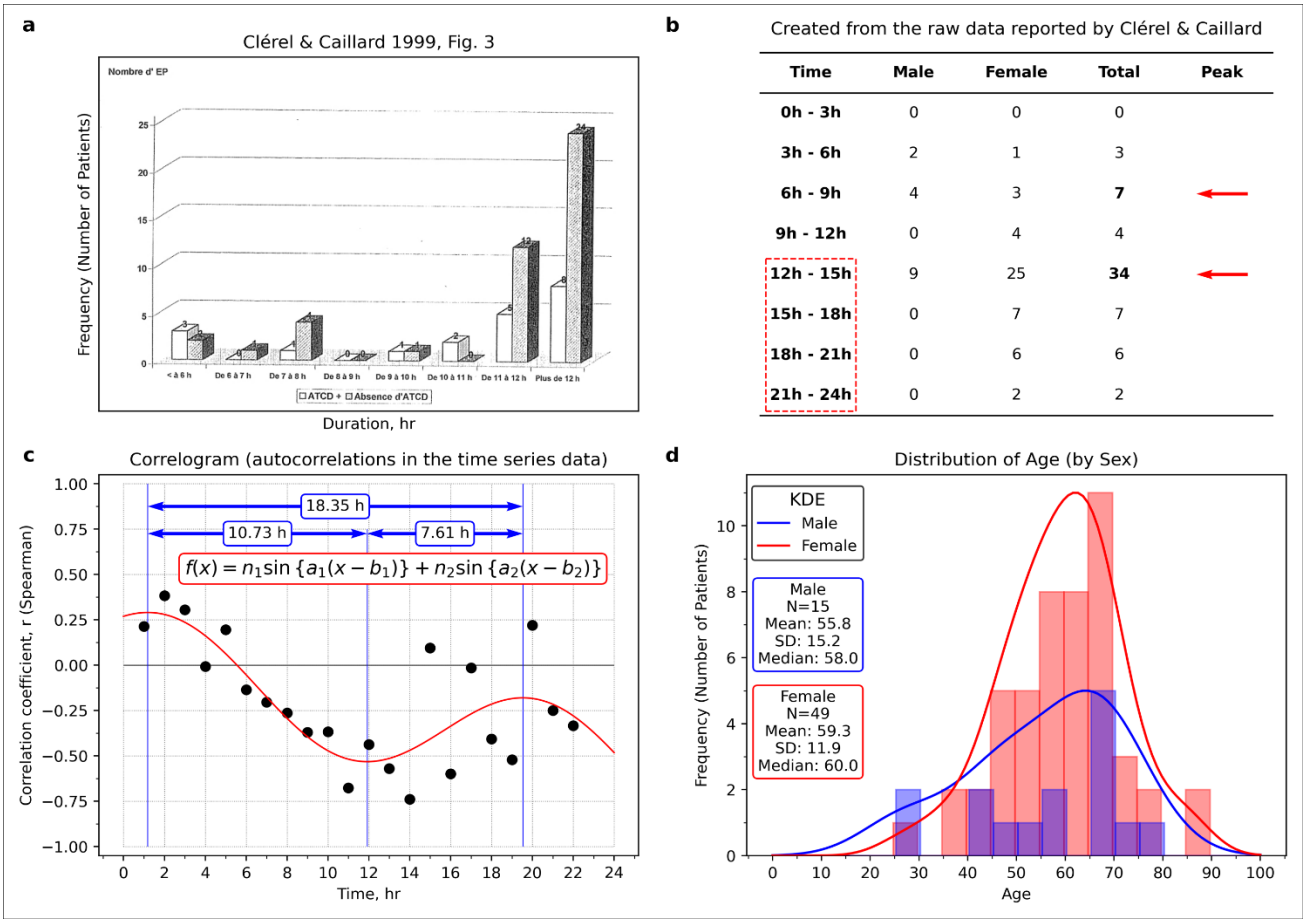

982

983 **Extended Data Fig. 4 | Re-analysis of the data in Table 1 by Clérel & Caillard[27]. a**, A figure made by

984 Clérel & Caillard[27] showed a relationship between travel time and the thrombosis onset in the case of

985 stratification by medical history of thrombosis. **b**, The relationship between time and thrombosis (prepared

986 from Table 1 reported by Clérel & Caillard[27]). **c**, Correlogram (prepared from Table 1 reported by Clérel &

987 Caillard[27]). **d**, Age distribution by sex (made from Table 1 reported by Clérel & Caillard[27]). As shown in panel

988 a, Clérel & Caillard[27] summarised all the data for 12 hours or more, but there were two peaks (see panel b).

989 Judging from the age distribution (panel d), the number of women patients was more significant than that of

men, but there was no difference between the age ranges. In panel c, there was a periodic pattern. Panel a reproduced from Clérel & Caillard. Syndrome thrombo-embolique de la station assise prolongée et vols de longue durée: l'expérience du Service Médical d'Urgence d'Aéroports De Paris. *Bull Acad Natl Med.* 1999; 183(5):985-997. discussion 997-1001. Figure 3.

997

998 **Extended Data Fig. 5**

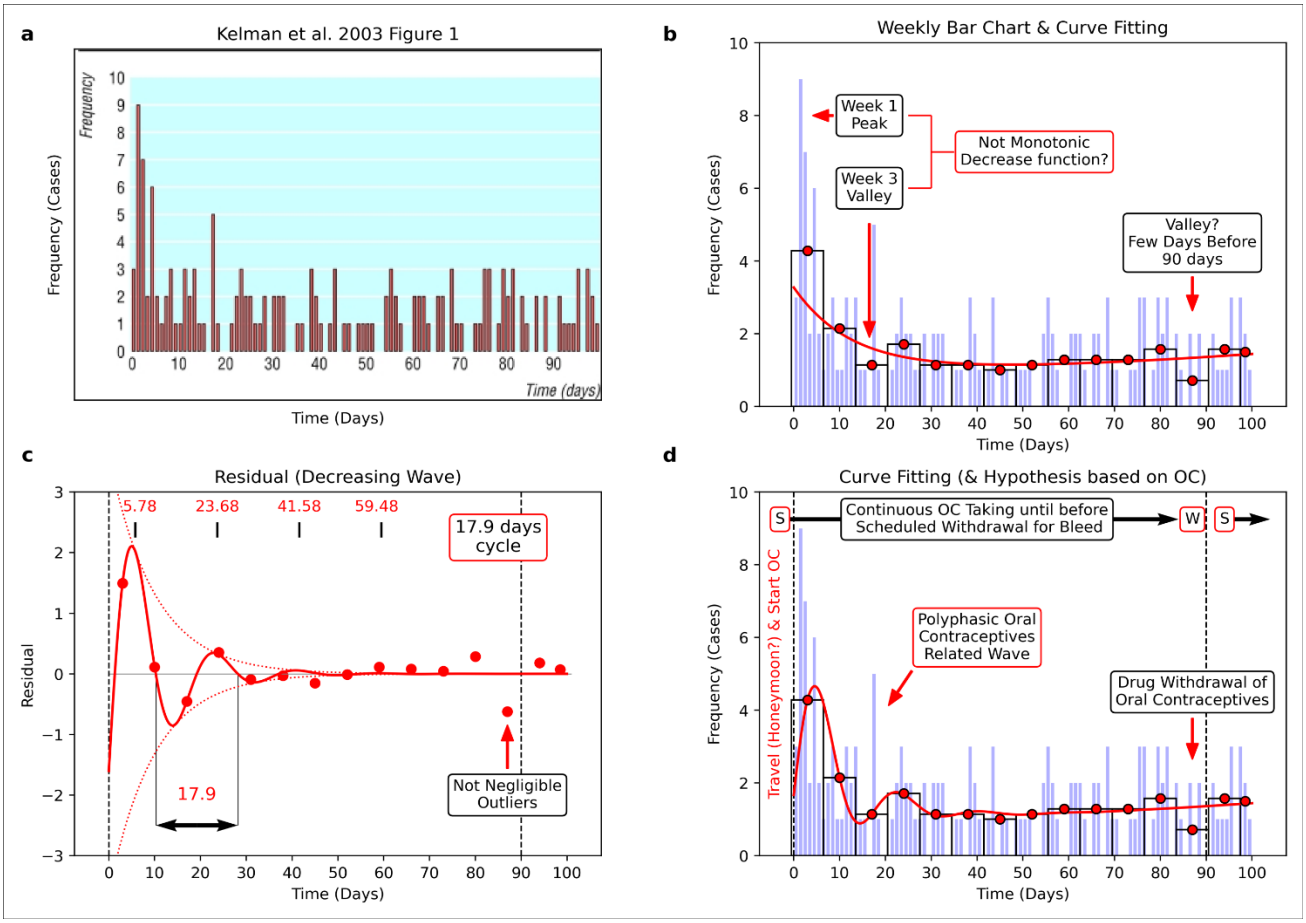

999

1000 **Extended Data Fig. 5 | Cyclic pattern of thrombosis onset appeared in a figure by Kelman et al[28]. a**, A

1001 thrombosis onset distribution reported by Kelman et al[28]. **b**, The regression curve is located in the centre of all

1002 average points (the points express the average of thrombosis onset during seven days). **c**, Curve fitting to the

1003 residual data of the regression curve in panel b. **d**, Application of damped wave function and adding

1004 interpretation of the results assuming some women started taking oral contraceptives (OC) in the timing of

1005 travel. The observed cyclic pattern was relatively unclear than Cannegieter et al.[25] **(see Fig. 2)**. Noteworthy,

1006 the thrombosis onset downed in the days before 90 days, and it seems to be the scheduled withdrawal period

of OC use. This figure was re-used and re-drawn from Kelman et al. *BMJ.* 2003; 327(7423):1072. Figure 1

https://www.ncbi.nlm.nih.gov/labs/pmc/articles/PMC261739/figure/fig1/

Extended Data Fig. 6

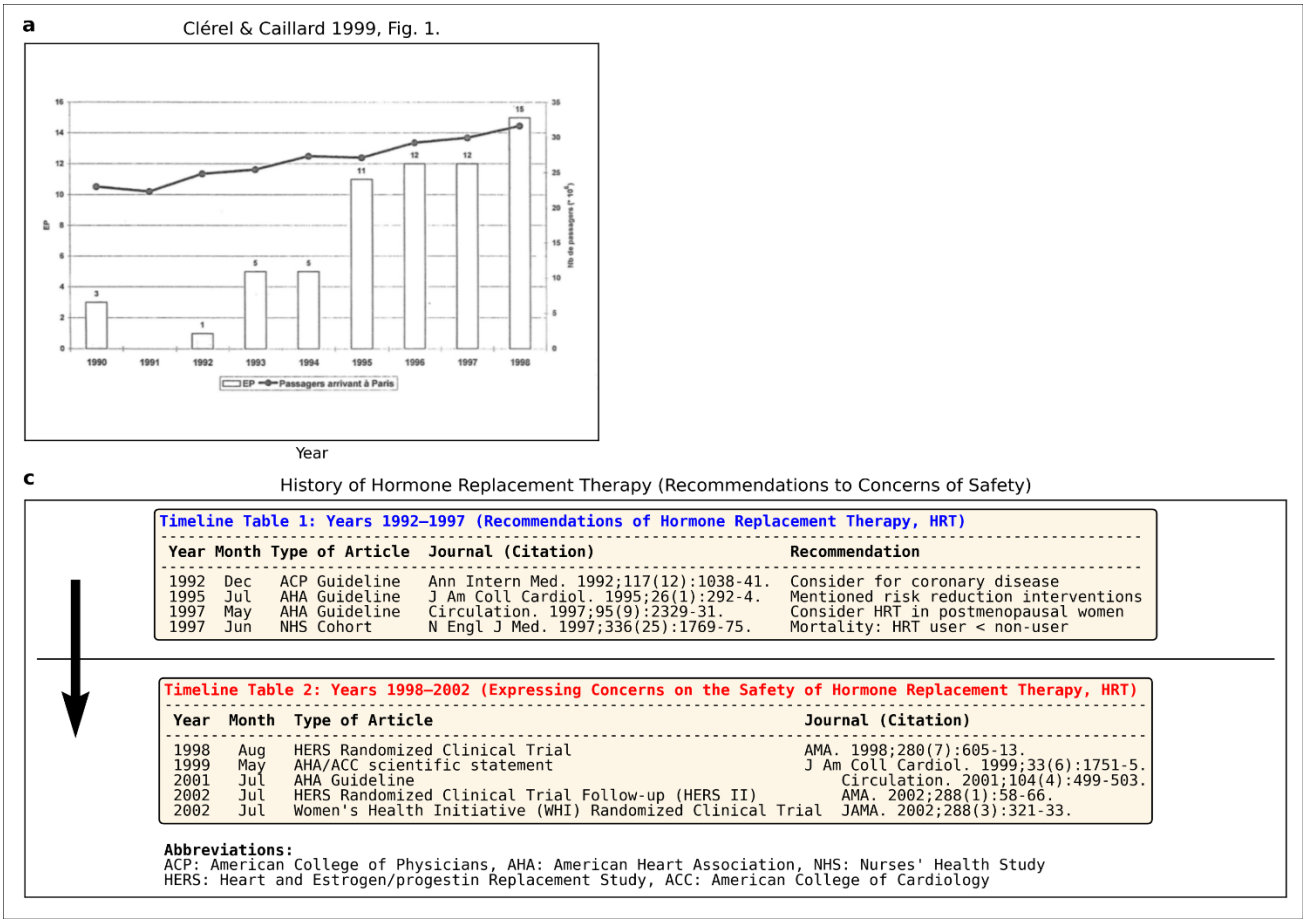

Extended Data Fig. 6 | Thrombosis reported by Clérel & Caillard[27] & our novel annotations. a, Clérel & Caillard mentioned that "their incidence increases during the last years, corresponding to the growth of air traffic and mainly to the increase of long duration without stop flight."[27] **c**, Chronology of various guidelines on HRT. In the newly figure (panel b), the increase in thrombosis was associated with the issuance time of guidelines for HRT. HRT was recommended for menopausal women in the 1990s, but its effectiveness was questioned in the HERS trial (1998)[31]. Also, the risk was discovered in the WHI trial at the interim analysis (2002)[32]. It might be the effect of the publication on the HERS study (1998)[31] that the increase of thromboses

was relatively small in 1998 despite the publication of two documents recommended in 1997. Panel a was reproduced from Clérel & Caillard. Syndrome thrombo-embolique de la station assise prolongée et vols de longue durée: l'expérience du Service Médical d'Urgence d'Aéroports De Paris. *Bull Acad Natl Med.* 1999; 183(5):985-997. discussion 997-1001. Figure 1.

Extended Data Fig. 7

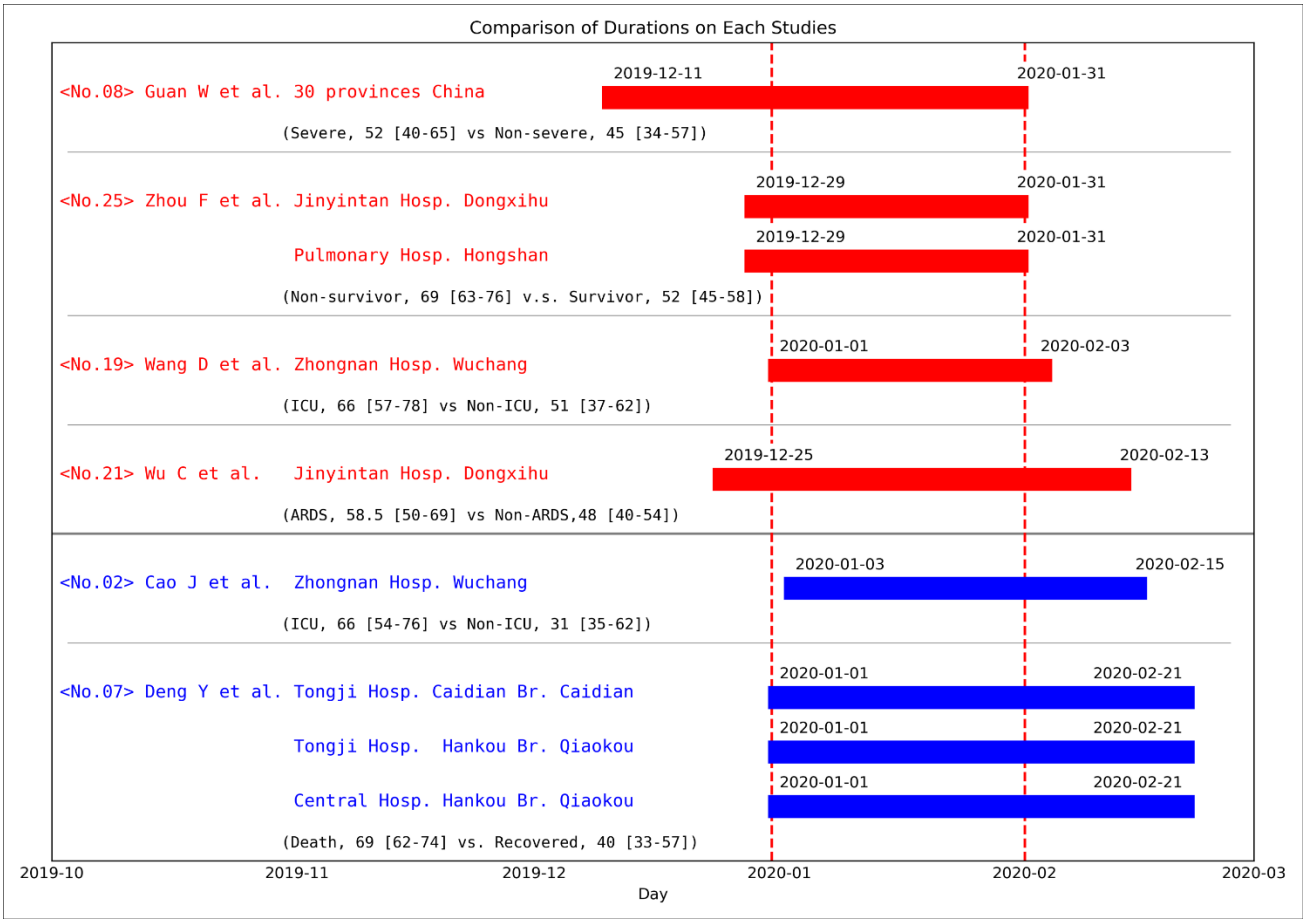

Extended Data Fig. 7 | Data cut-off dates in each study cited by Matsushita et al[33]. The data acquisition period in each study was displayed in Gantt chart format. The date display format is year-month-day. The correspondence between numbers and authors is as follows: **No.2**: Cao et al. (Cao, J. et al., *Intensive Care Med.* 2020;46(5):851-853.)[59], **No.7**: Deng et al. (Deng, Y. et al., *Chin Med J (Engl).* 2020;133(11):1261-1267.)[60], **No.8**: Guan et al. (Guan, W.J. et al., *N Engl J Med.* 2020;382(18):1708-1720.)[61], **No.19**: Wang D. et al. (Wang, D. et al., *JAMA.* 2020;323(11):1061-1069.)[62], **No.20**: Wang L. et al. (Wang, L. et al., *J Infect.* 2020;80(6):639-645.)[63], **No.21**: Wu et al. (Wu, C. et al., *JAMA Intern Med.* 2020;180(7):934-943.)[64], **No.25**:

Zhou et al. (Zhou, F. et al., *Lancet.* 2020;395(10229):1054-1062.)[66]. Abbreviations: ARDS (Acute Respiratory Distress Syndrome), ICU (Intensive Care Unit). The number in parentheses means median age. The number in the bracket means standard deviation or interquartile range.

1044 **Extended Data Fig. 8**

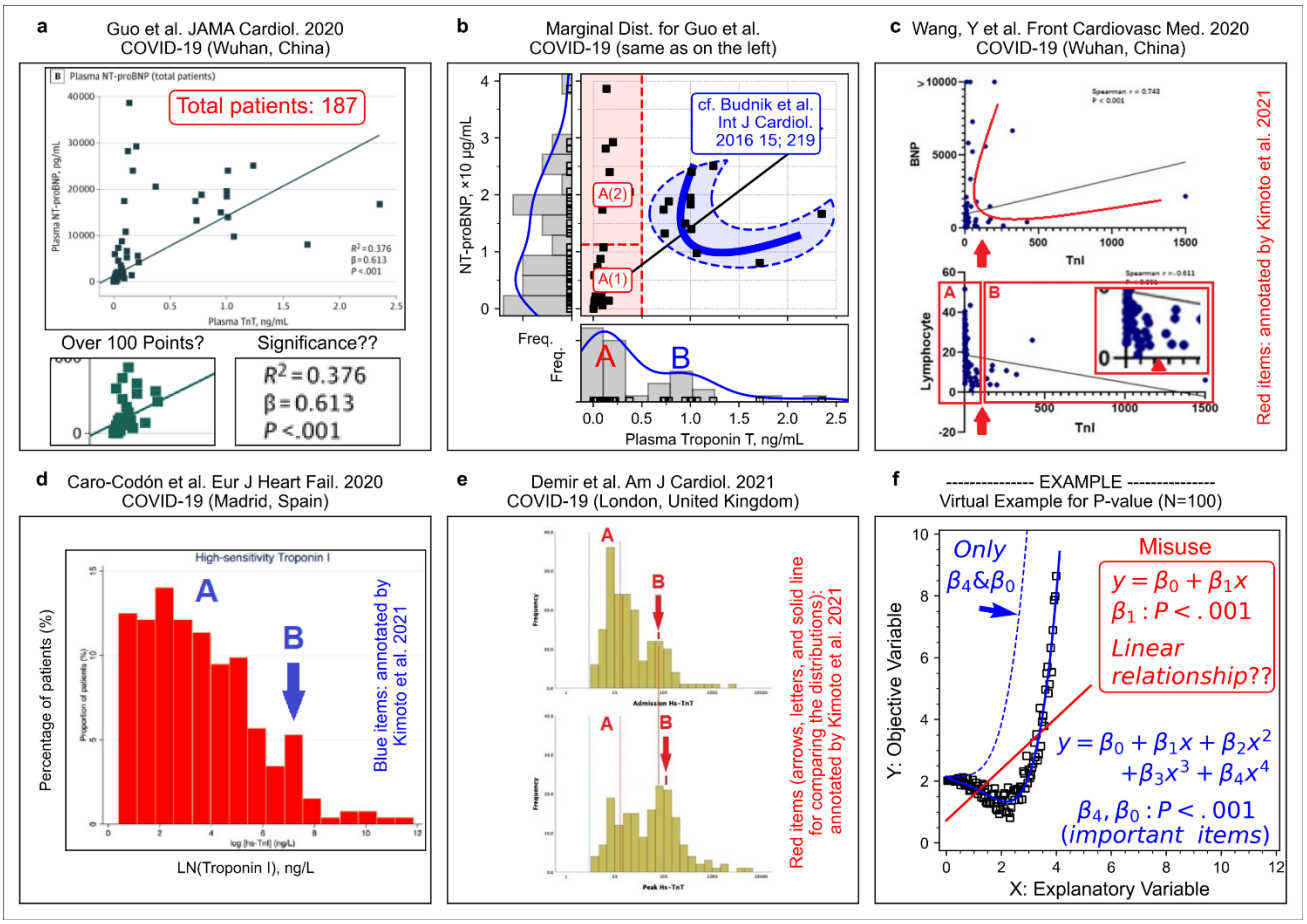

1045

1046 **Extended Data Fig. 8 | Bimodal distributions & tiled parabola in COVID-19 patients. a,** Guo et al. *JAMA*

1047 *Cardiol.* 2020; 5(7):811-818. Figure 1B

1048 https://www.ncbi.nlm.nih.gov/labs/pmc/articles/PMC7101506/figure/hoi200026f1/

1049 Copyright © 2020 Guo T et al. JAMA Cardiology. Creative Commons Attribution License (CC-BY). **b,**

1050 Marginal distribution of the scatter plot data. **c,** Wang et al. *Front Cardiovasc Med.* 2020; (7): 147. Figure 1

1051 (upper, x-axis: troponin I, pg/mL; y-axis: BNP, pg/mL; lower, x-axis: troponin I, pg/mL; y-axis:

1052 lymphocyte, %)[37]. https://www.ncbi.nlm.nih.gov/labs/pmc/articles/PMC7477309/figure/F1/

1053 Copyright © 2020 Wang, Zheng, Tong, Wang, Lv, Xi and Liu. CC BY License. **d,** Caro-Codón et al. *Eur J*

1054 *Heart Fail.* 2021; 23(3):456-464. Figure 1B (x-axis, LN (troponin I))[40].

1055 https://www.ncbi.nlm.nih.gov/labs/pmc/articles/PMC8013330/figure/ejhf2095-fig-0001/

1056 Copyright © 2021 European Society of Cardiology. All rights reserved. This Figure can be used for

1057 unrestricted research re-use and analysis in any form or by any means with acknowledgement of the original

1058 source as part of the COVID-19 public health emergency, for the duration of the emergency. **e,** Demir et al.

1059 *Am J Cardiol.* 2021; 147:129-136. Figure 2 (upper: admission; lower: peak measurements; x-axis: troponin T,

1060 ng/L)[41]. https://www.ncbi.nlm.nih.gov/labs/pmc/articles/PMC7895690/figure/fig0002/

1061 Copyright © 2021 Elsevier Inc. All rights reserved. This figure is granted for unrestricted research re-use and

1062 analyses in any form or by any means with acknowledgement of the original source by Elsevier for as long as

1063 the COVID-19 resource centre remains active. **f,** Virtual example on regression analysis (**see Supplementary**

1064 **discussion 5: misuse of linear regression analysis**). In panel b (also c, d, and e), the histogram was bimodal

1065 (marked "A" and "B"). The crescent-shape pattern closely resembled the ST-segment elevation myocardial

1066 infarction group pattern that appeared in the study by Budnik et al[36].

1067

1068

Extended Data Fig. 9

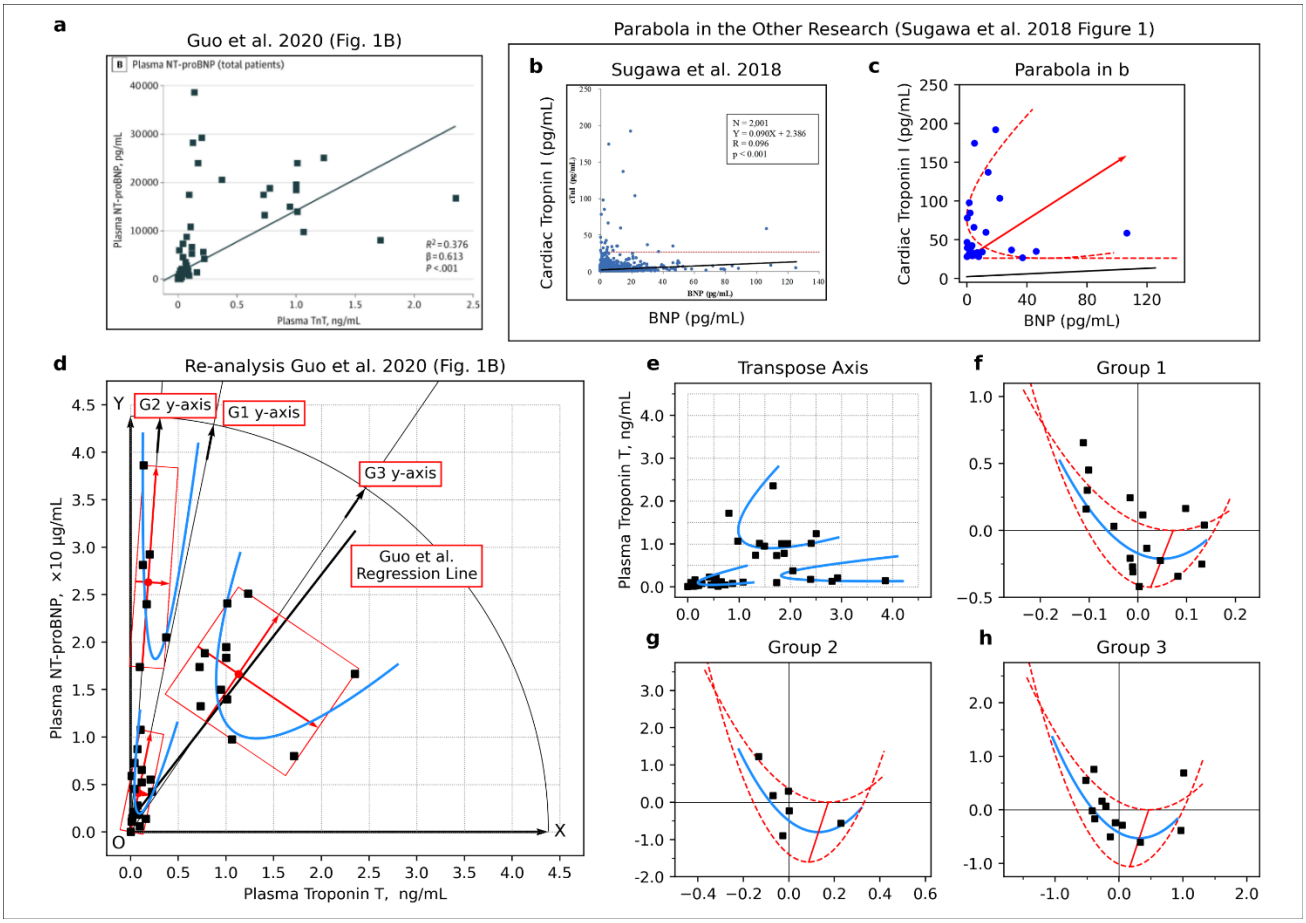

Extended Data Fig. 9 | Three subgroup patterns appeared in a figure reported by Guo et al[35]. a, A scatter plot showing the relationship between cardiac troponin T (TnT) and N-terminal pro-brain natriuretic peptide (NT-proBNP) in a patient with COVID-19[35]. **b**, Scatter plot to investigate the relationship between brain natriuretic peptide (BNP) and cardiac troponin I (cTnI) in healthy subjects reported by Sugawa et al[38]. **c**, The visible points that exceeded the value of 26.2 pg/mL (red line in panel b) were re-plotted with parabola (not accurate regression analysis). **d**, Visible points in the figure reported by Guo et al.[35] with parabolas. **e**, Transposed panel d for easy comparison. **f**, Group 1 in the small coordinate system (centre of gravity as the

origin of the coordinate system). **g**, Group 2 in the small coordinate system. **h**, Group 3 in the small coordinate system. In panel f-h, the upper curve is expressed by a quadratic function, in which a coefficient of the quadratic term is equal to a value of the coefficient of the quadratic term for the solid curve multiplied by 3/2. In the lower curve, a coefficient of the quadratic term of the solid curve multiplied by 2/3. Most data points located inside the crescent-shaped region enclosed by the parabolas, but the reason was unclear. Panel a was re-used from Guo T et al. *JAMA Cardiol.* 2020; 5(7):811-818. Figure 1B https://www.ncbi.nlm.nih.gov/labs/pmc/articles/PMC7101506/figure/hoi200026f1/ Copyright © 2020 Guo T et al. JAMA Cardiology. Creative Commons Attribution License (CC-BY). https://creativecommons.org/licenses/by/4.0/ Panel b was re-used from Sugawa et al. *Sci Rep.* 2018; 8(1):5120. Figure 1. https://www.ncbi.nlm.nih.gov/labs/pmc/articles/PMC5865159/figure/Fig1/ Copyright © 2018 The Authors. CC-BY 4.0 License

Extended Data Fig. 10

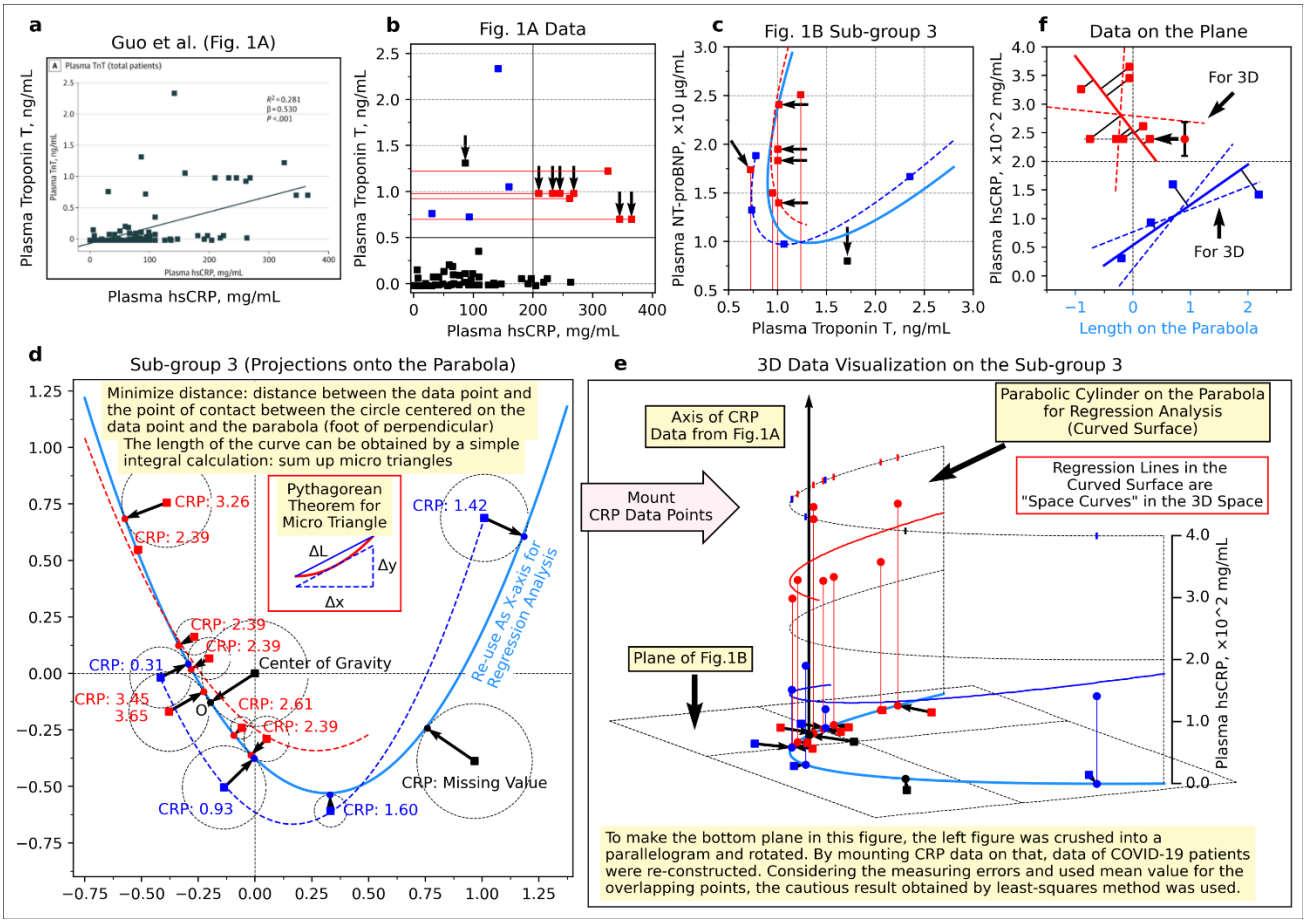

Extended Data Fig. 10 | A three-dimensional plot reconstructed from the data reported by Guo et al[35]. **a**, Scatter plot showing the relationship between high sensitive C-reactive protein (hsCRP) and troponin T (TnT) [35]. **b**, Re-drawn scatter plot with a vertical line around hsCRP = 200 mg/mL = 2.0 × 10^2 mg/mL. **c**, Enlarged subgroup 3 in the panel d of Extended Data Fig. 9 (data exceeding hsCRP = 200 mg/mL are indicated by red, data not exceeding hsCRP = 200 mg/mL are indicated by blue). **d**, Enlarged subgroup 3 of the panel d in Extended Fig. 9 with the foot of the perpendicular from each data point to the parabola. **e**, The hsCRP value of each patient placed on panel d (shown as a three-dimensional plot). **f**, The side surface of the

parabolic cylinder. The point of TnT = 1.31 observed in panel b is not included in panel c, and the point of TnT = 1.71 in panel c is not included in panel b (inconsistent). In panel e, the projection of the data points onto the parabola was used as new points. In panels, e and f, some points of CRP value could not be determined because of overlapping, so those points were replaced with the average value (the points indicated by the left-pointing arrows and the error bar, which are the average values and the range of values, respectively). Panel a was re-used from Guo et al. *JAMA Cardiol.* 2020; 5(7):811-818. Figure 1. https://www.ncbi.nlm.nih.gov/labs/pmc/articles/PMC7101506/figure/hoi200026f1/